

Electronic Supplementary Information

**Reactions of chalcogens and borane with phosphazane macrocycles derived
from diethanolamine and P₂N₂ building blocks †**

Manu Goyal, Chandrakala Negi, Nitish Kumar Garg, Shalender Jain and Sanjay Singh*

*Corresponding Author: sanjaysingh@iisermohali.ac.in

Department of Chemical Sciences, Indian Institute of Science Education and Research Mohali, Knowledge City, Sector 81, SAS Nagar, Mohali 140306, Punjab, India.

Table of contents

1. Heteronuclear NMR Spectra of Compounds 1-10.....	3
2. Crystal Data and Refinement Details of Compounds 1-3, 8 and 9.....	24
3. References.....	

26

1. Heteronuclear NMR Spectra of Compounds 1-10

Heteronuclear NMR spectra of $[\{P(\mu\text{-}N^t\text{Bu})\}_2\{O(CH_2)_2N(Me)(CH_2)_2O\}]_2$ (1)

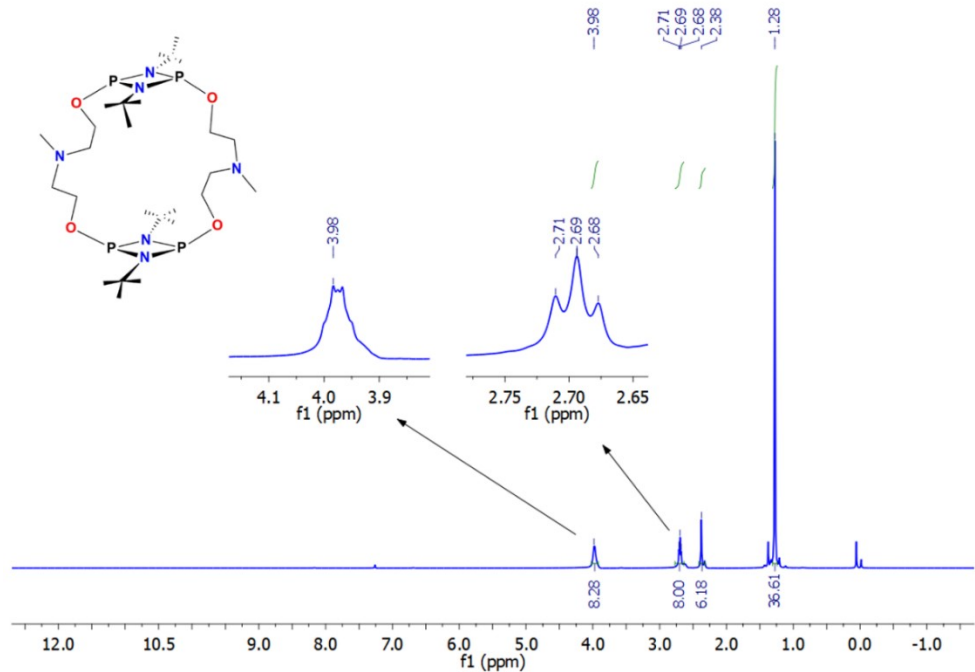


Fig.S1 ^1H NMR (400 MHz, CDCl_3) spectrum of $[\{P(\mu\text{-}N^t\text{Bu})\}_2\{O(CH_2)_2N(Me)(CH_2)_2O\}]_2$ (1).

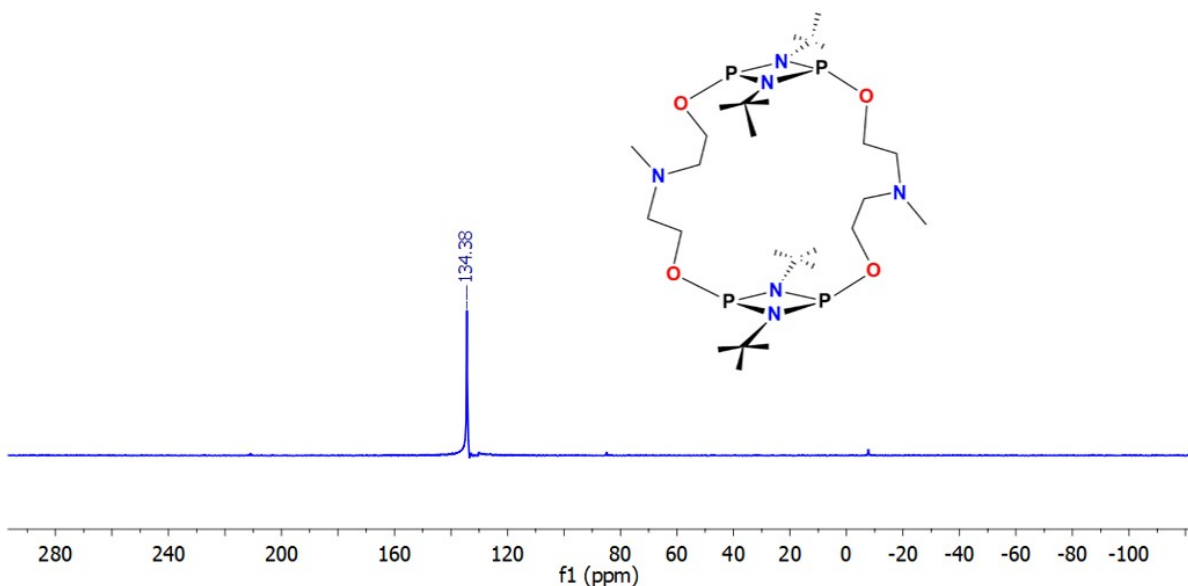


Fig.S2 $^{31}\text{P}\{\text{H}\}$ NMR (162MHz, CDCl_3) spectrum of $[\{P(\mu\text{-}N^t\text{Bu})\}_2\{O(CH_2)_2N(Me)(CH_2)_2O\}]_2$ (1).

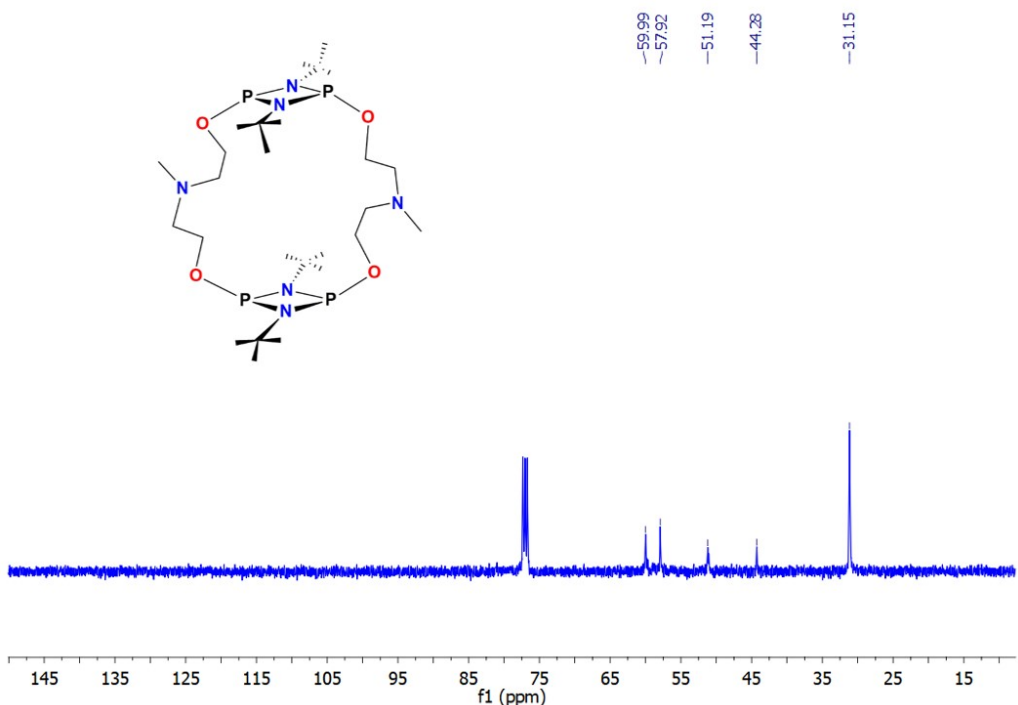


Fig.S3 $^{13}\text{C}\{\text{H}\}$ NMR (100 MHz, CDCl_3) spectrum of $[\{\text{P}(\mu\text{-N}^t\text{Bu})\}_2\{\text{O}(\text{CH}_2)_2\text{N}(\text{Me})(\text{CH}_2)_2\text{O}\}]_2$ (**1**).

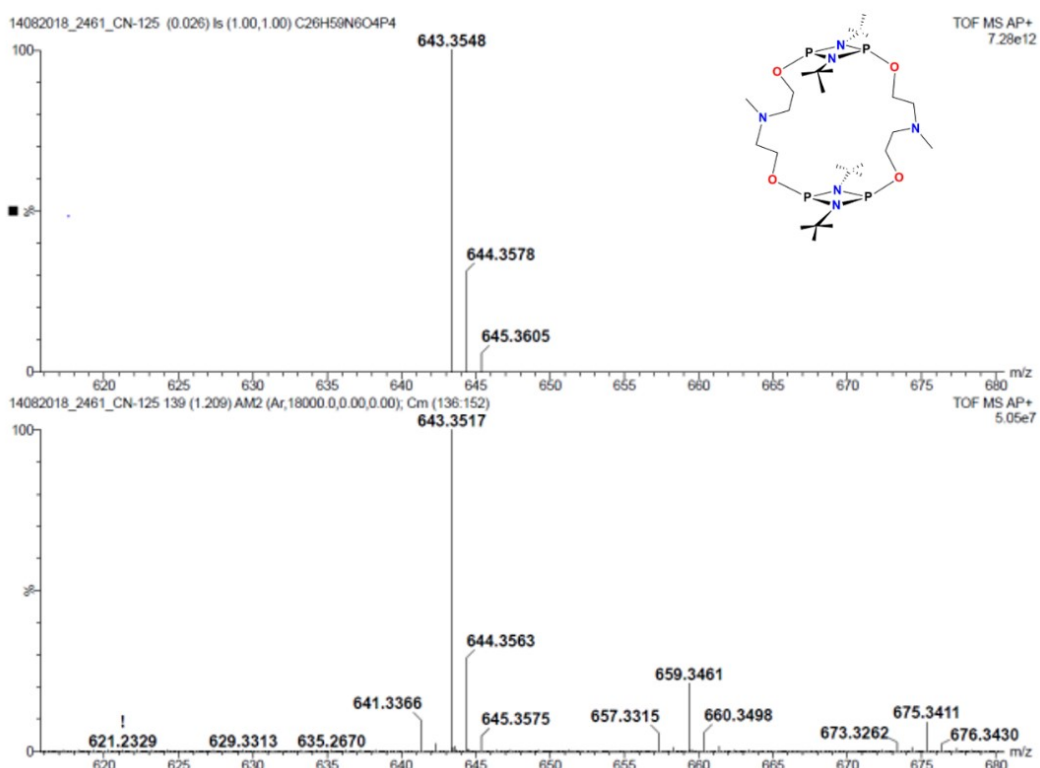


Fig.S4 HRMS spectrum of $[\{\text{P}(\mu\text{-N}^t\text{Bu})\}_2\{\text{O}(\text{CH}_2)_2\text{N}(\text{Me})(\text{CH}_2)_2\text{O}\}]_2$ (**1**).

Heteronuclear NMR spectra of $\left[\{P(\mu-N^tBu)\}_2\{O(CH_2)_2N(Ph)(CH_2)_2O\}\right]_2$ (2)

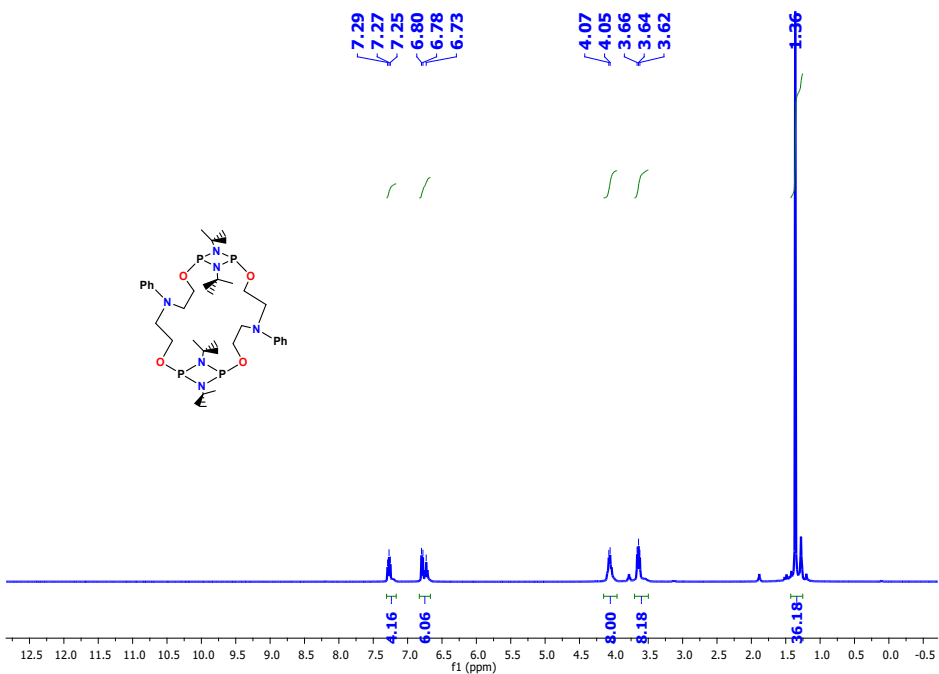


Fig.S5 ^1H NMR (400 MHz, CDCl_3) spectrum of $[\{\text{P}(\mu\text{-N}^t\text{Bu})\}_2\{\text{O}(\text{CH}_2)_2\text{N}(\text{Ph})(\text{CH}_2)_2\text{O}\}]_2$ (2).

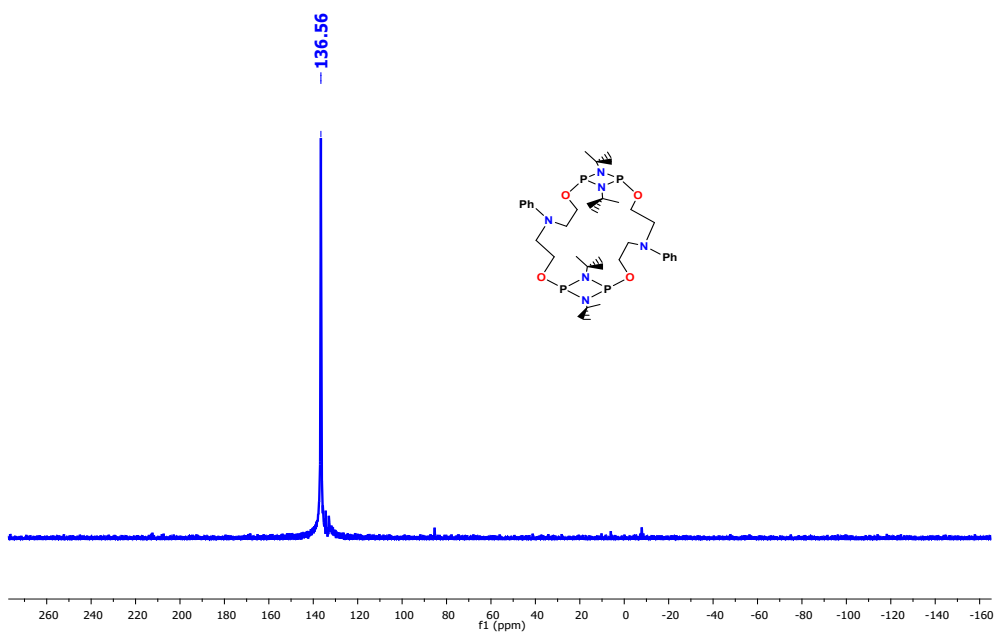


Fig.S6 $^{31}\text{P}\{\text{H}\}$ NMR (162 MHz, CDCl_3) spectrum of $[\{\text{P}(\mu\text{-N}^t\text{Bu})\}_2\{\text{O}(\text{CH}_2)_2\text{N}(\text{Ph})(\text{CH}_2)_2\text{O}\}]_2$ (2).

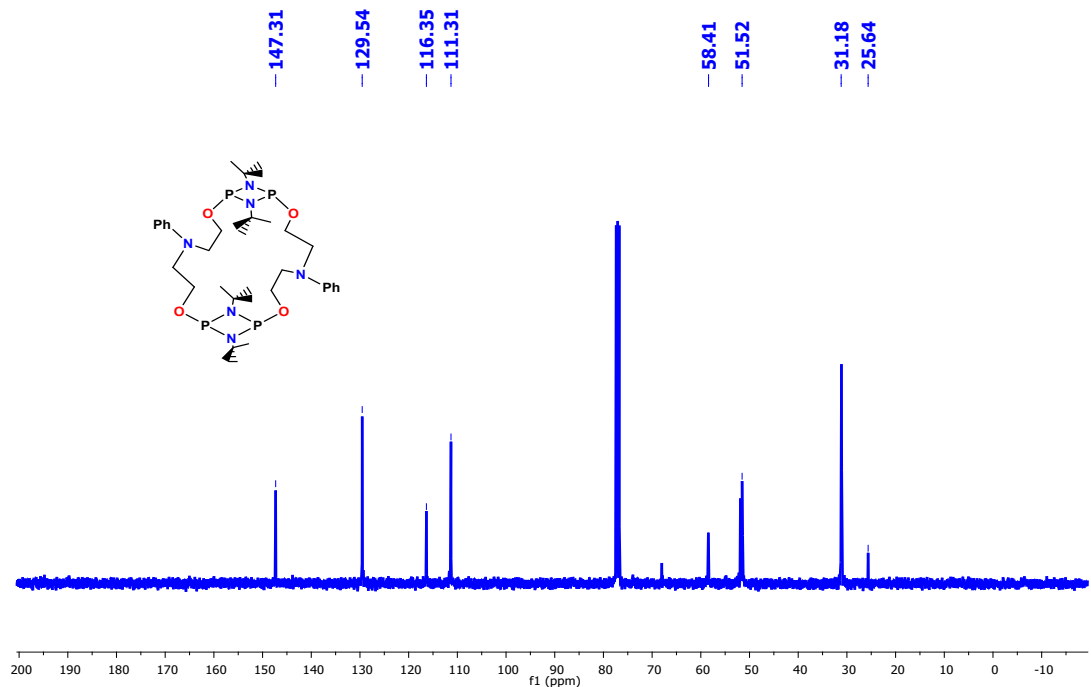


Fig.S7 $^{13}\text{C}\{\text{H}\}$ NMR (100 MHz, CDCl_3) spectrum of $[\{\text{P}(\mu\text{-N}^t\text{Bu})\}_2\{\text{O}(\text{CH}_2)_2\text{N}(\text{Ph})(\text{CH}_2)_2\text{O}\}]_2$ (**2**).

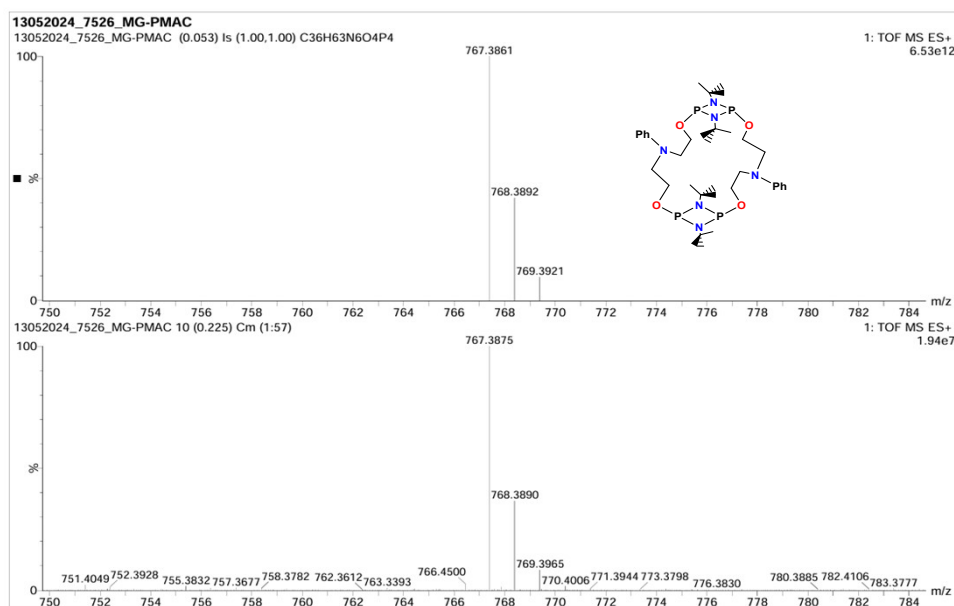


Fig.S8 HRMS spectrum of $[\{\text{P}(\mu\text{-N}^t\text{Bu})\}_2\{\text{O}(\text{CH}_2)_2\text{N}(\text{Ph})(\text{CH}_2)_2\text{O}\}]_2$ (**2**).

Heteronuclear NMR spectra of $[\{\text{O}=\text{P}(\mu\text{-N}^t\text{Bu})\}_2\{\text{O}(\text{CH}_2)_2\text{N}(\text{Me})(\text{CH}_2)_2\text{O}\}]_2$ (**3**)

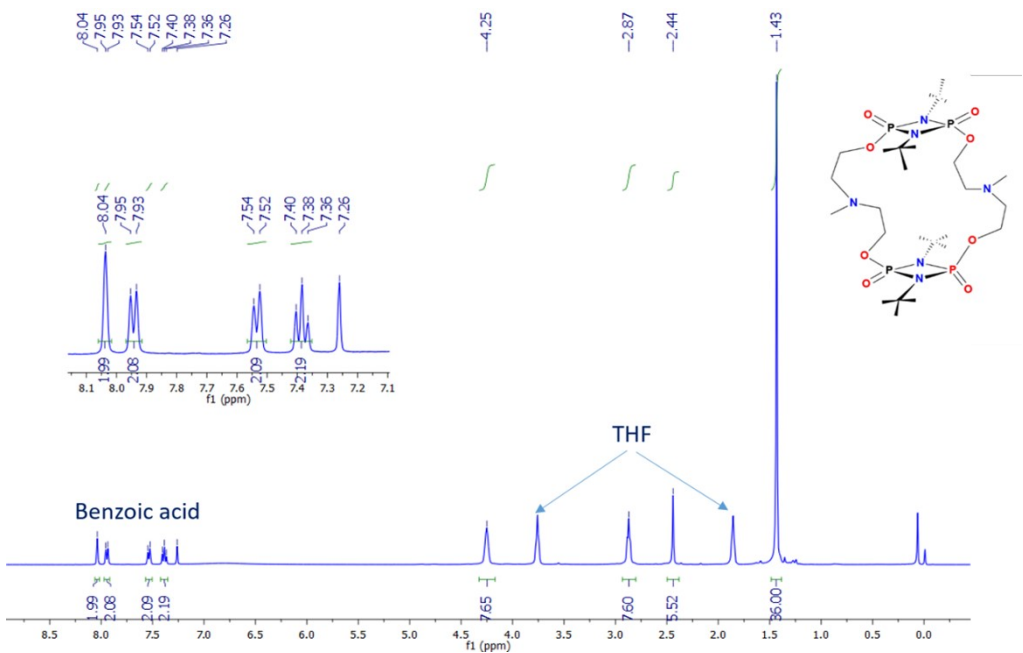


Fig. S9 ^1H NMR (400 MHz, CDCl_3) of $[\{\text{(O=)P}(\mu\text{-N}^t\text{Bu})\}_2\{\text{O}(\text{CH}_2)_2\text{N}(\text{Me})(\text{CH}_2)_2\text{O}\}]_2$ (**3**).

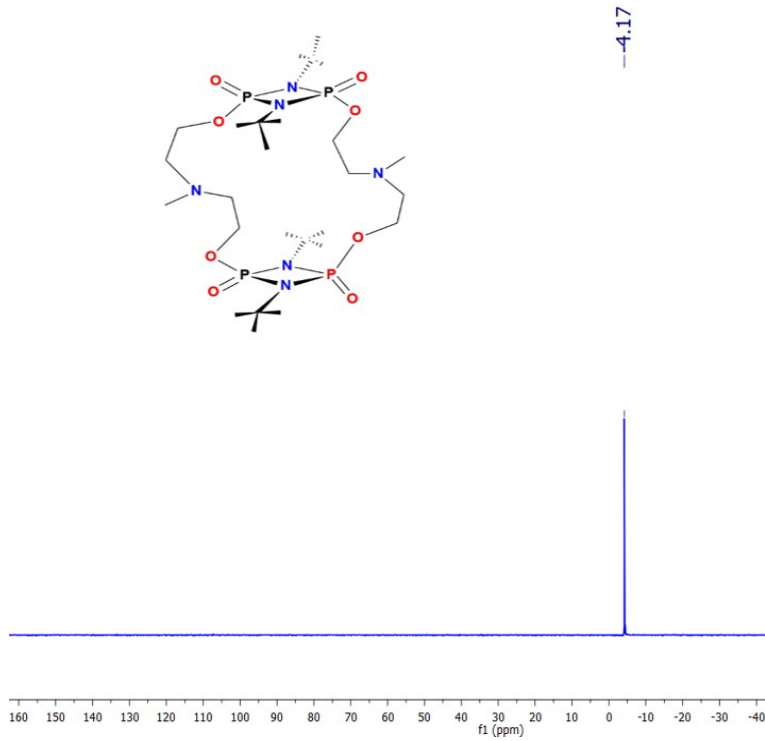


Fig. S10 $^{31}\text{P}\{\text{H}\}$ NMR (162 MHz, CDCl_3) of $[\{\text{(O=)P}(\mu\text{-N}^t\text{Bu})\}_2\{\text{O}(\text{CH}_2)_2\text{N}(\text{Me})(\text{CH}_2)_2\text{O}\}]_2$ (**3**).

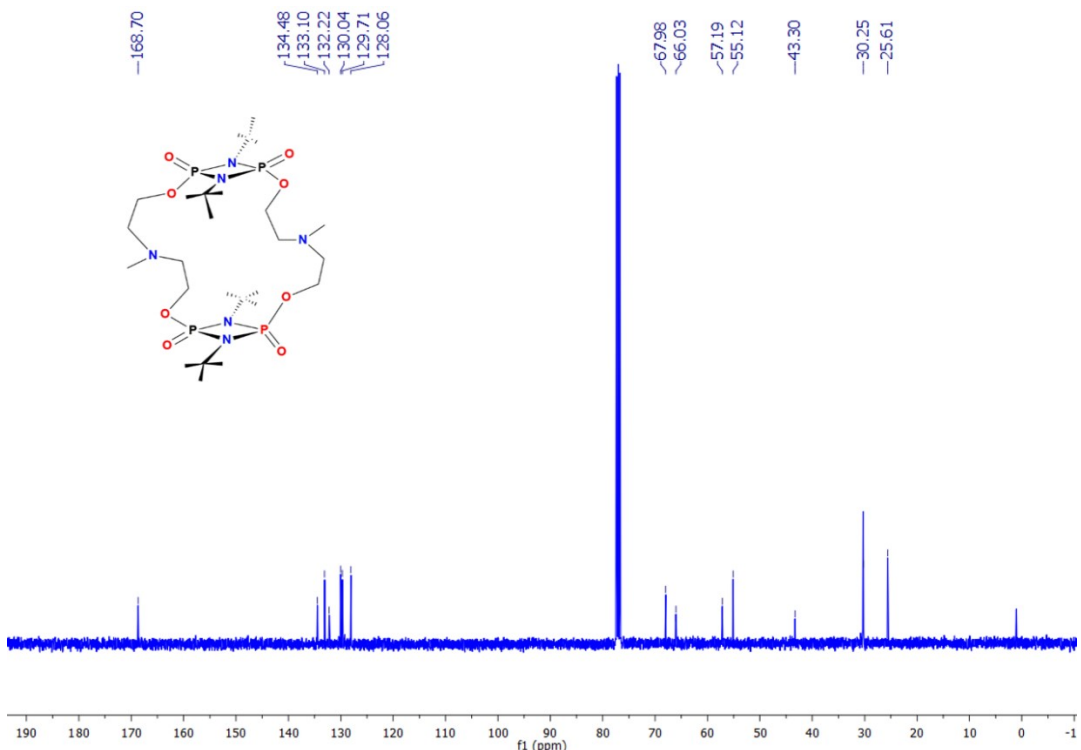


Fig. S11 $^{13}\text{C}\{\text{H}\}$ NMR (100 MHz, CDCl_3) of $[\{(O=)\text{P}(\mu\text{-N}^t\text{Bu})\}_2\{\text{O}(\text{CH}_2)_2\text{N}(\text{Me})(\text{CH}_2)_2\text{O}\}]_2$ (**3**).

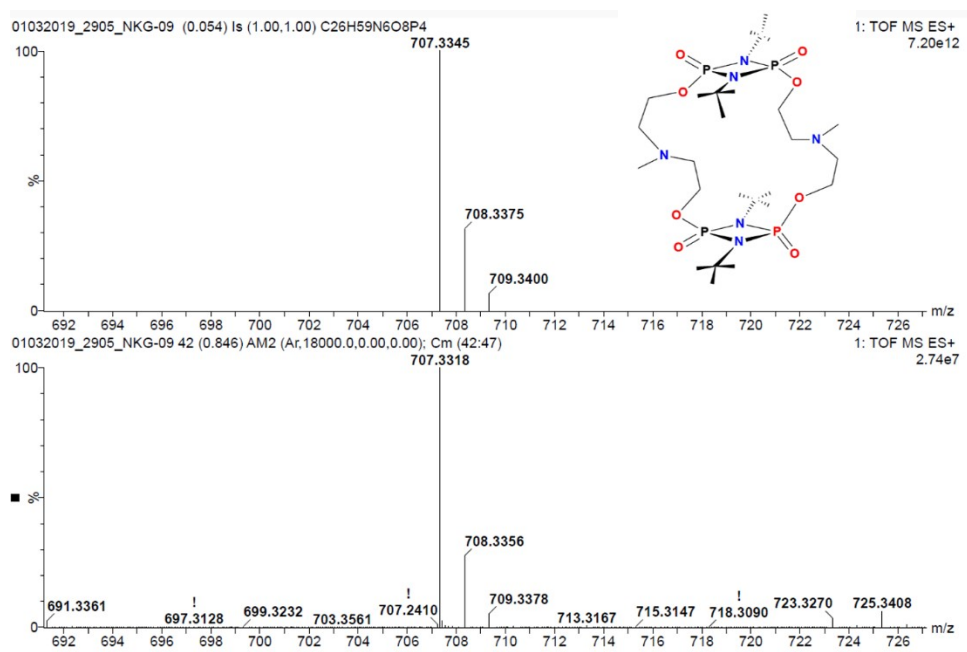


Fig. S12 HRMS of $[\{(O=)\text{P}(\mu\text{-N}^t\text{Bu})\}_2\{\text{O}(\text{CH}_2)_2\text{N}(\text{Me})(\text{CH}_2)_2\text{O}\}]_2$ (**3**).

Heteronuclear NMR spectra of $\left[\{(O=)P(\mu-N^tBu)\}_2\{O(CH_2)_2N(Ph)(CH_2)_2O\}\right]_2$ (4)

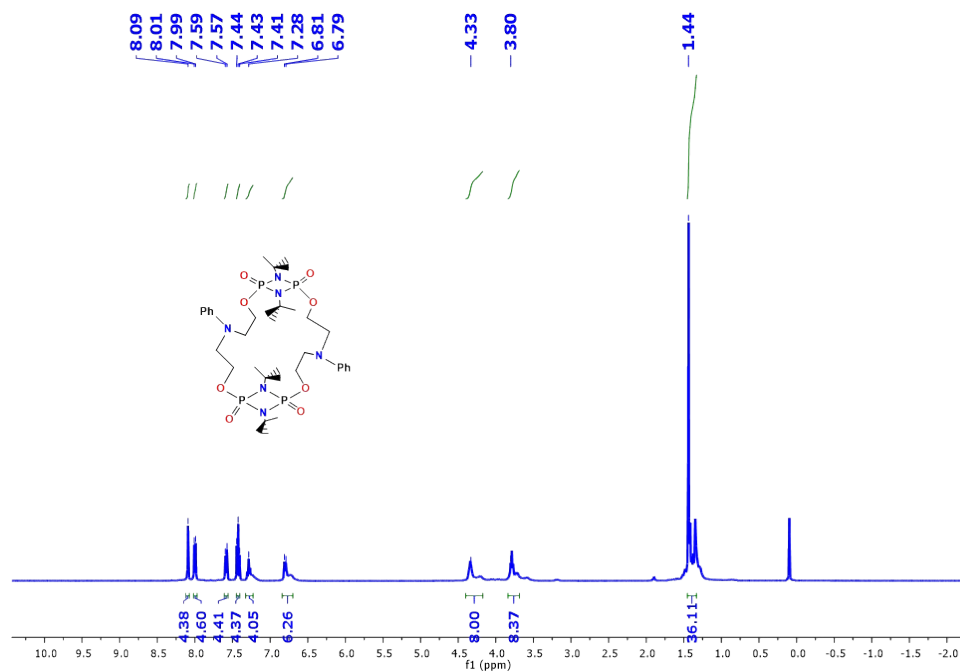


Fig.S13 ^1H NMR (400 MHz, CDCl_3) spectrum of $\left[\{(O=)P(\mu-N^tBu)\}_2\{O(CH_2)_2N(Ph)(CH_2)_2O\}\right]_2$ (4).

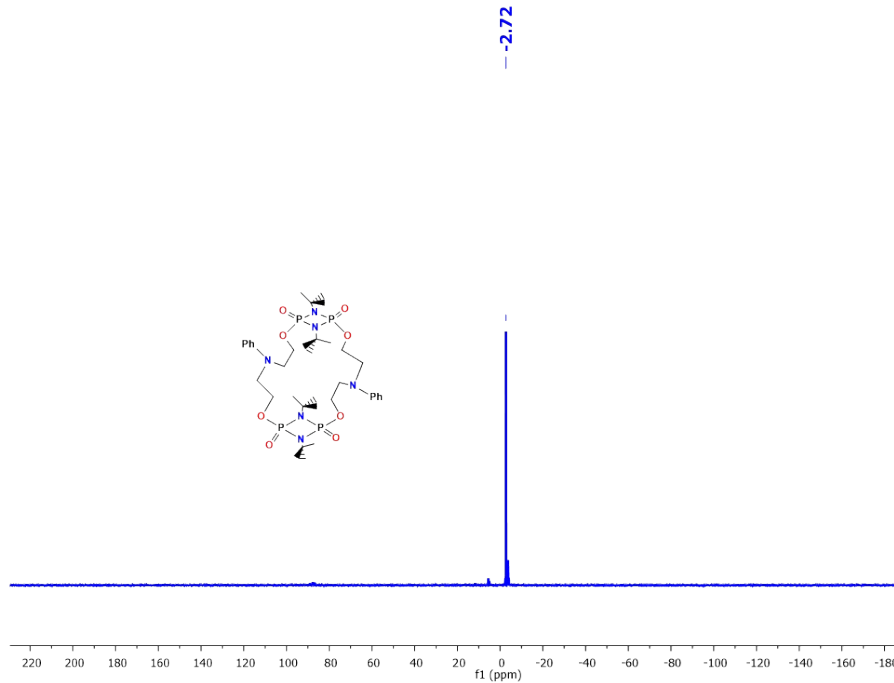


Fig.S14 $^{31}\text{P}\{\text{H}\}$ NMR (162 MHz, CDCl_3) spectrum of $\left[\{(O=)P(\mu-N^tBu)\}_2\{O(CH_2)_2N(Ph)(CH_2)_2O\}\right]_2$ (4).

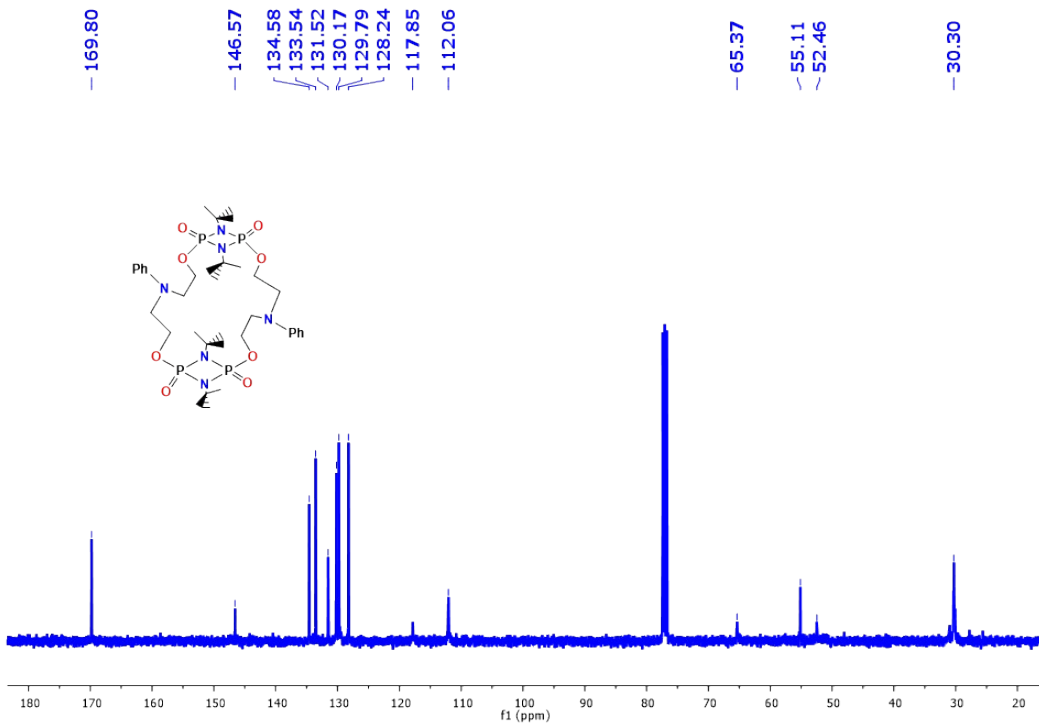


Fig.S15 $^{13}\text{C}\{^1\text{H}\}$ NMR (100 MHz, CDCl_3) spectrum of $[\{(O=)\text{P}(\mu\text{-N}^t\text{Bu})\}_2\{\text{O}(\text{CH}_2)_2\text{N}(\text{Ph})(\text{CH}_2)_2\text{O}\}]_2$ (**4**).

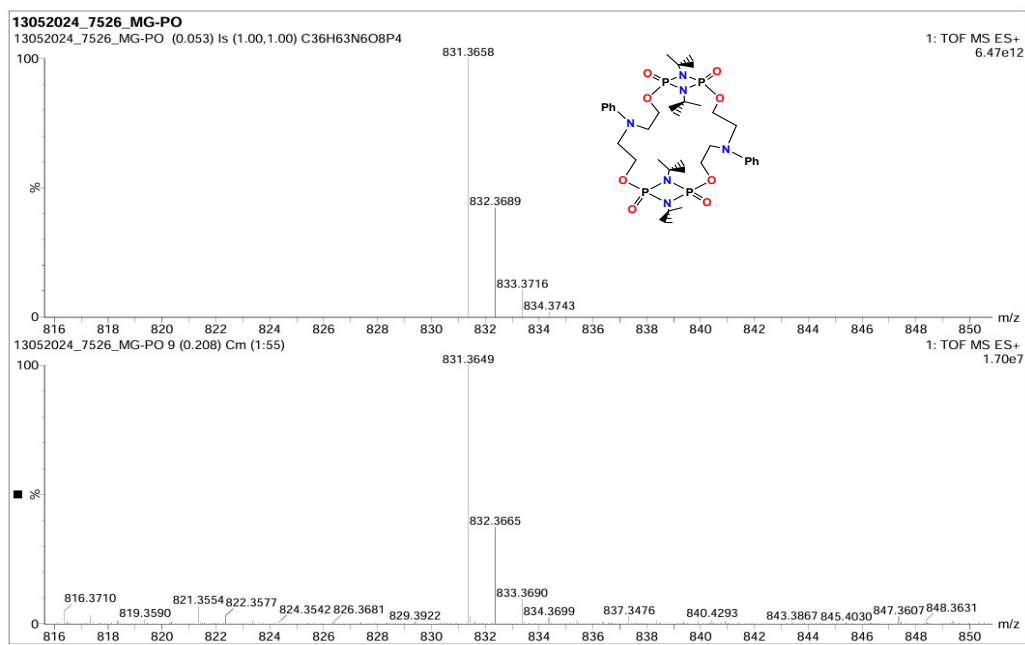


Fig.S16 HRMS spectrum of $[\{(O=)\text{P}(\mu\text{-N}^t\text{Bu})\}_2\{\text{O}(\text{CH}_2)_2\text{N}(\text{Ph})(\text{CH}_2)_2\text{O}\}]_2$ (**4**).

Heteronuclear NMR spectra of $\left[\{(S=)P(\mu-N^tBu)\}_2\{O(CH_2)_2N(Me)(CH_2)_2O\}\right]_2$ (5)

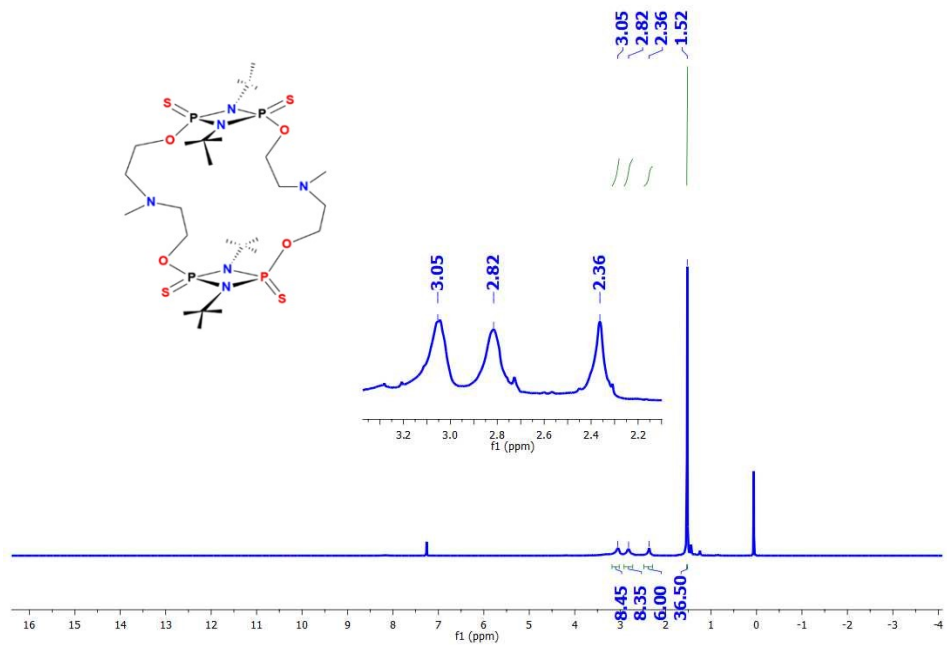


Fig. S17 ^1H NMR (400 MHz, C_6D_6) spectrum of $\left[\{(S=)P(\mu-N^tBu)\}_2\{O(CH_2)_2N(Me)(CH_2)_2O\}\right]_2$ (5).

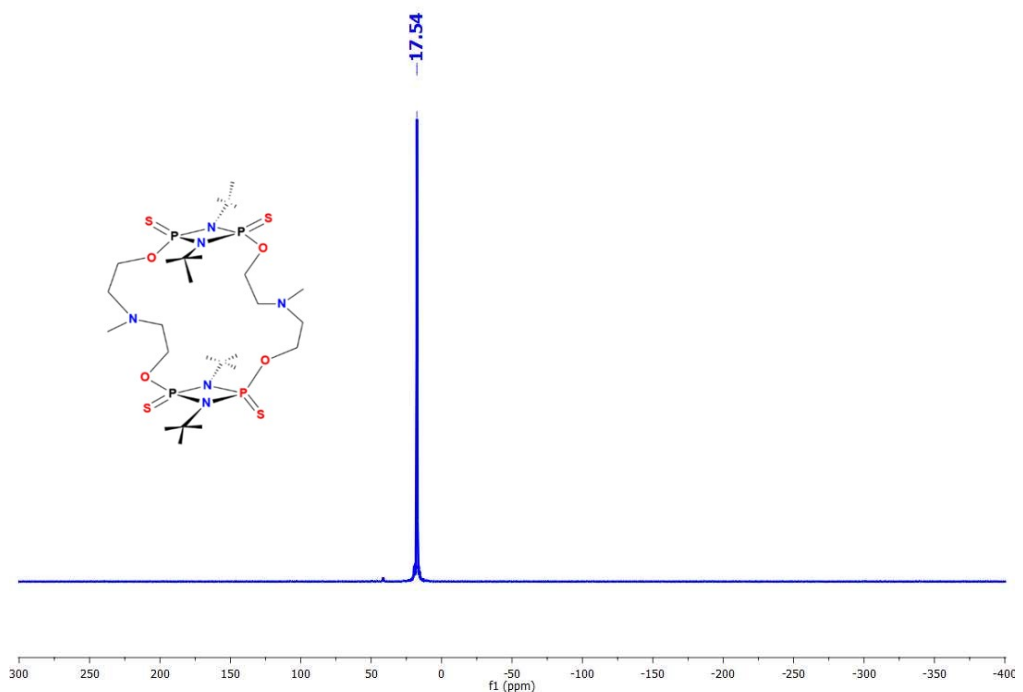


Fig.S18 $^{31}\text{P}\{\text{H}\}$ NMR (162 MHz, C_6D_6) spectrum of $\left[\{(S=)P(\mu-N^tBu)\}_2\{O(CH_2)_2N(Me)(CH_2)_2O\}\right]_2$ (5).

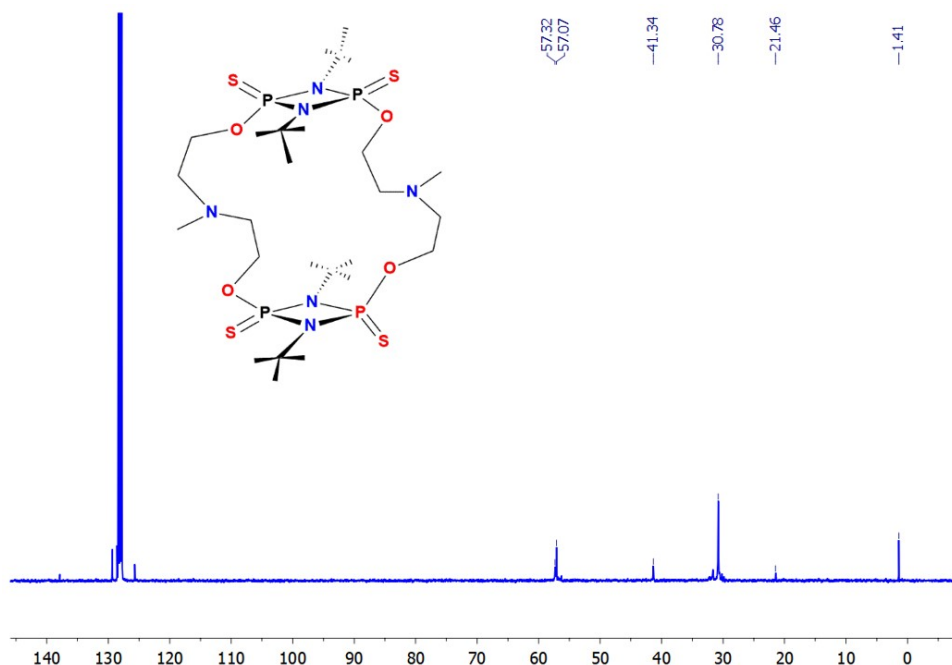


Fig.S19 $^{13}\text{C}\{\text{H}\}$ NMR (100 MHz, C_6D_6) spectrum of $[\{(S=)\text{P}(\mu\text{-N}^t\text{Bu})\}_2\{\text{O}(\text{CH}_2)_2\text{N}(\text{Me})(\text{CH}_2)_2\text{O}\}]_2$ (**5**).

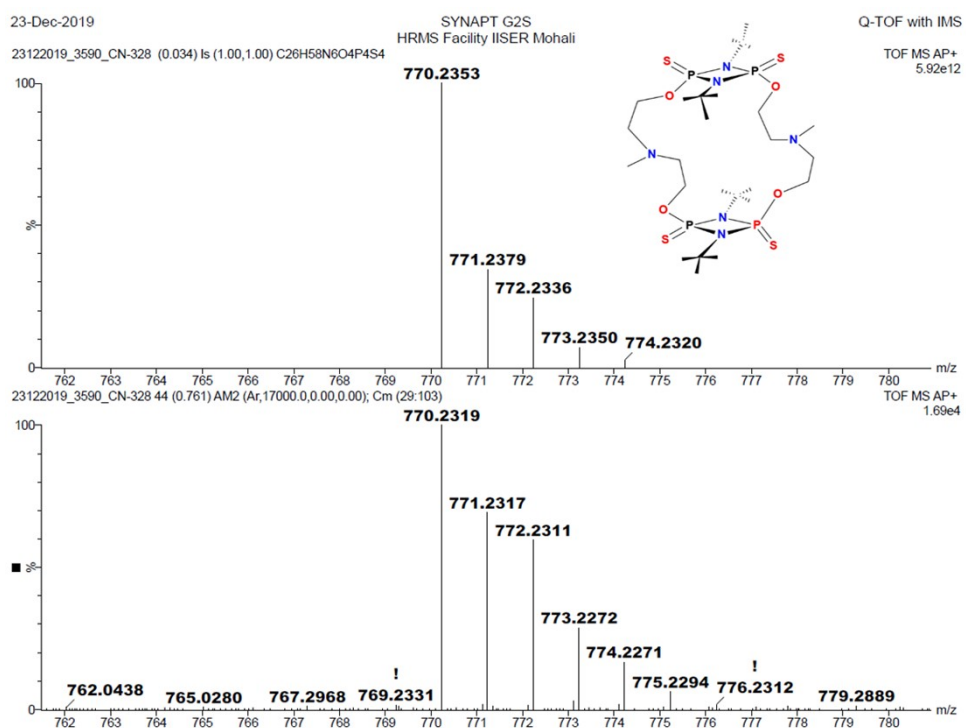


Fig.S20 HRMS spectrum of $[\{(S=)\text{P}(\mu\text{-N}^t\text{Bu})\}_2\{\text{O}(\text{CH}_2)_2\text{N}(\text{Me})(\text{CH}_2)_2\text{O}\}]_2$ (**5**).

Heteronuclear NMR spectra of $[\{(S=)P(\mu\text{-}N^tBu)\}_2\{O(CH_2)_2N(Ph)(CH_2)_2O\}]_2$ (6)

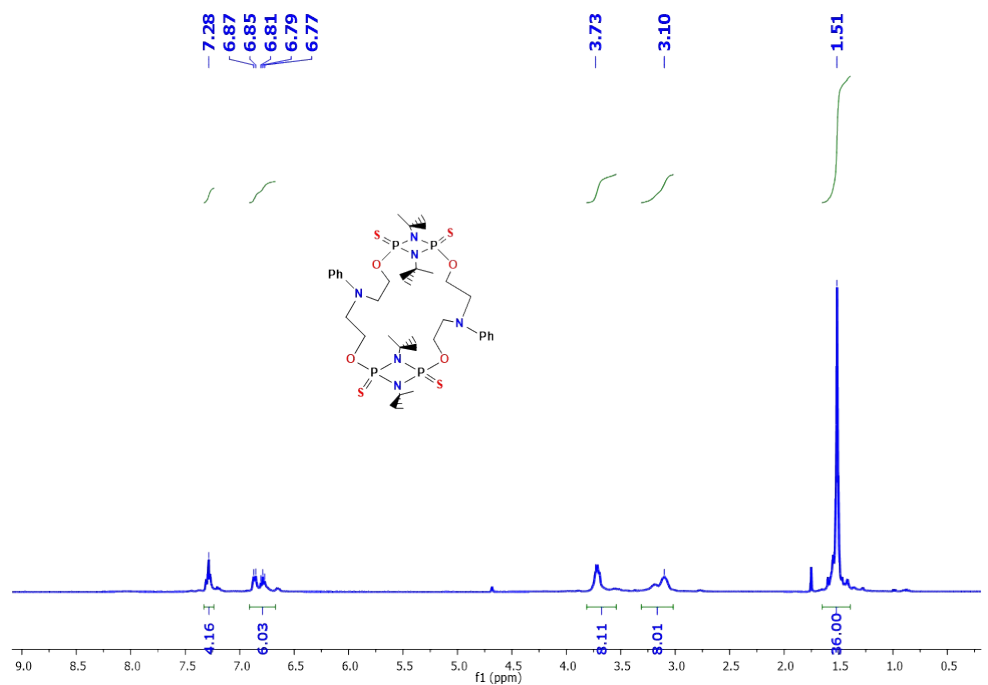


Fig.S21 1H NMR (400 MHz, $CDCl_3$) spectrum of $[\{(S=)P(\mu\text{-}N^tBu)\}_2\{O(CH_2)_2N(Ph)(CH_2)_2O\}]_2$ (6).

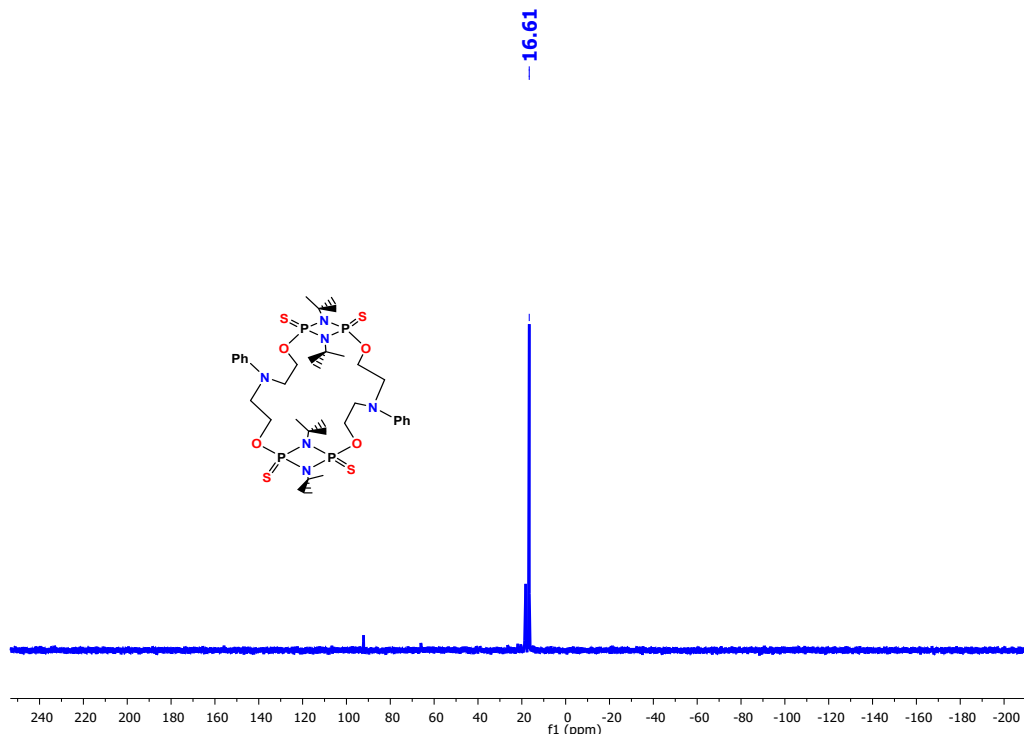


Fig.S22 $^{31}P\{^1H\}$ NMR (162 MHz, $CDCl_3$) spectrum of $[\{(S=)P(\mu\text{-}N^tBu)\}_2\{O(CH_2)_2N(Ph)(CH_2)_2O\}]_2$ (6).

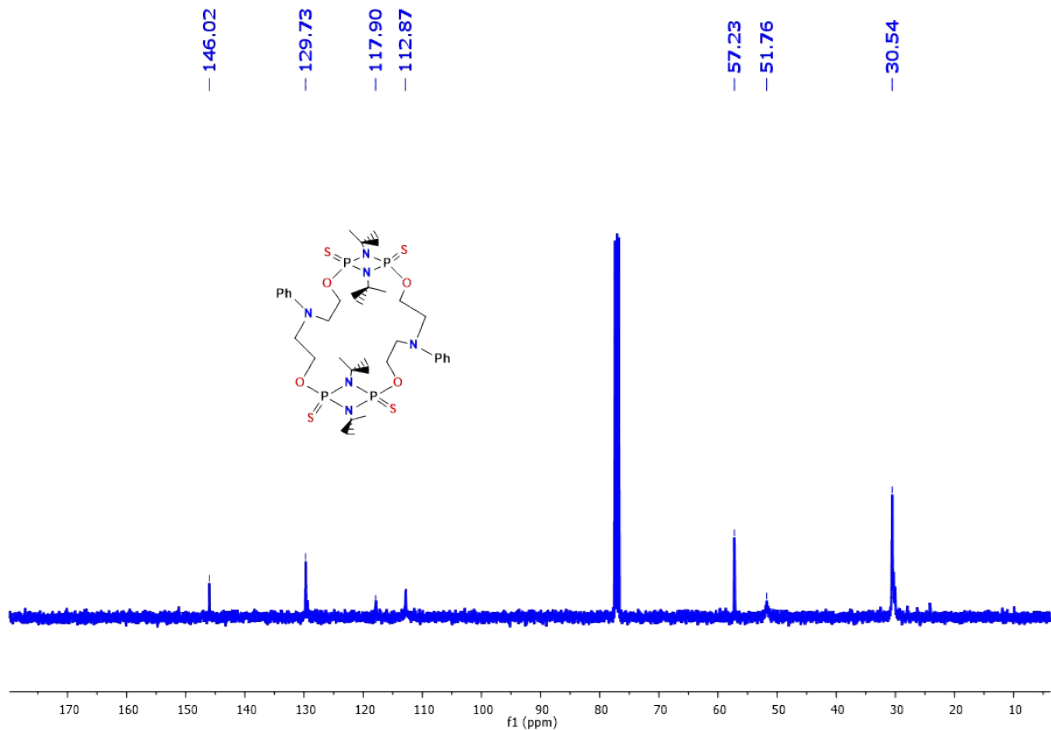


Fig.S23 $^{13}\text{C}\{^1\text{H}\}$ NMR (100 MHz, CDCl_3) spectrum of $[\{(S=)\text{P}(\mu\text{-N}^t\text{Bu})\}_2\{\text{O}(\text{CH}_2)_2\text{N}(\text{Ph})(\text{CH}_2)_2\text{O}\}]_2$ (**6**).

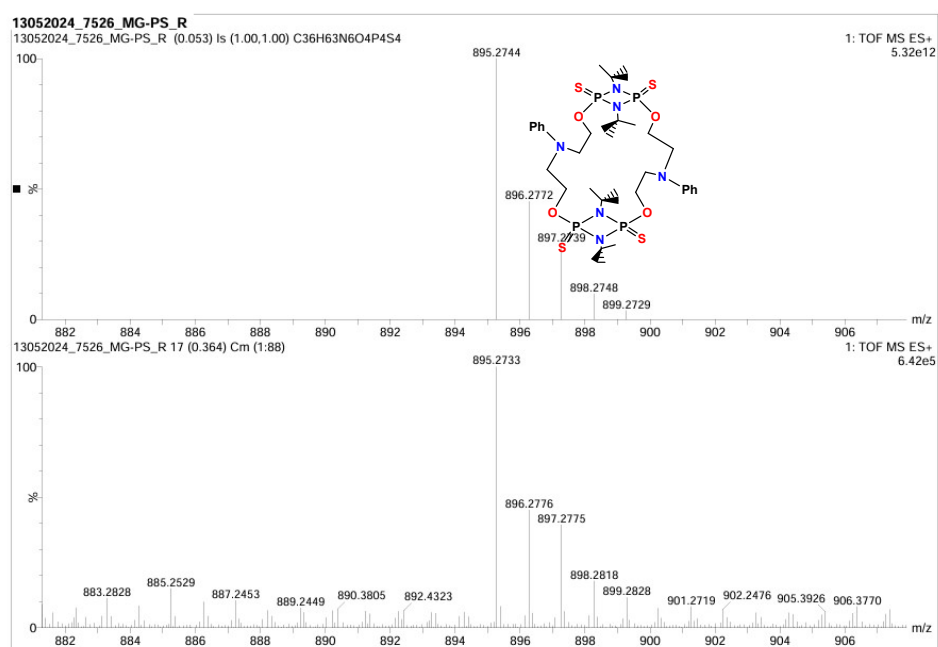


Fig.S24 HRMS spectrum of $[\{(S=)\text{P}(\mu\text{-N}^t\text{Bu})\}_2\{\text{O}(\text{CH}_2)_2\text{N}(\text{Ph})(\text{CH}_2)_2\text{O}\}]_2$ (**6**).

Heteronuclear NMR spectra of $\{(\text{Se}=\text{P}(\mu\text{-N}^t\text{Bu})_2\}\}_2\{\text{O}(\text{CH}_2)_2\text{N}(\text{Me})(\text{CH}_2)_2\text{O}\}_2$ (7)

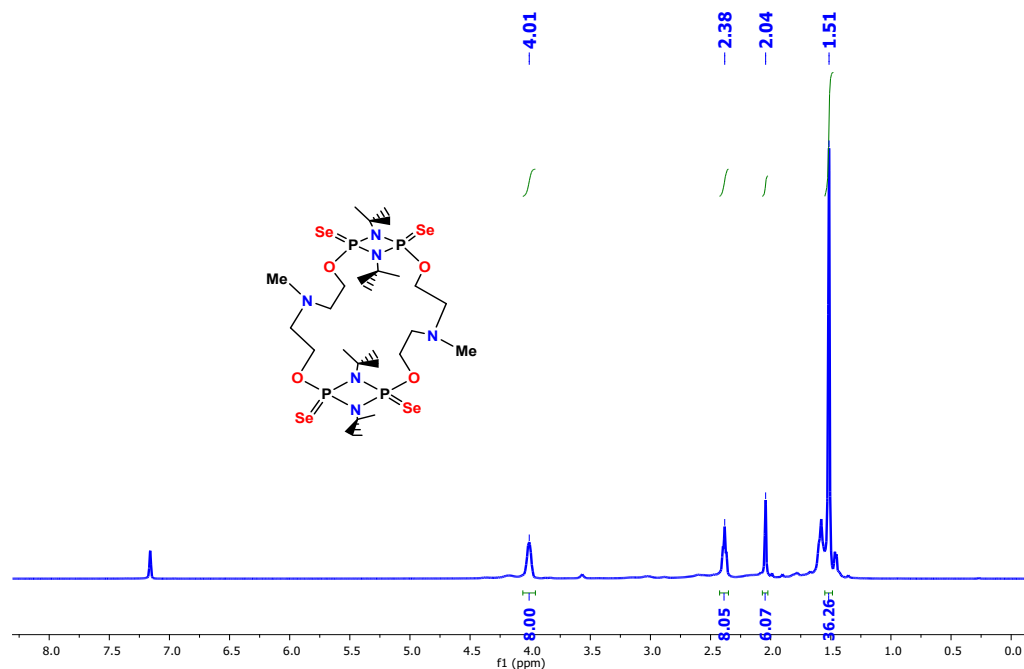


Fig. S25 ^1H NMR (400 MHz, C_6D_6) spectrum of $\{(\text{Se}=\text{P}(\mu\text{-N}^t\text{Bu})_2\}\}_2\{\text{O}(\text{CH}_2)_2\text{N}(\text{Me})(\text{CH}_2)_2\text{O}\}_2$ (7).

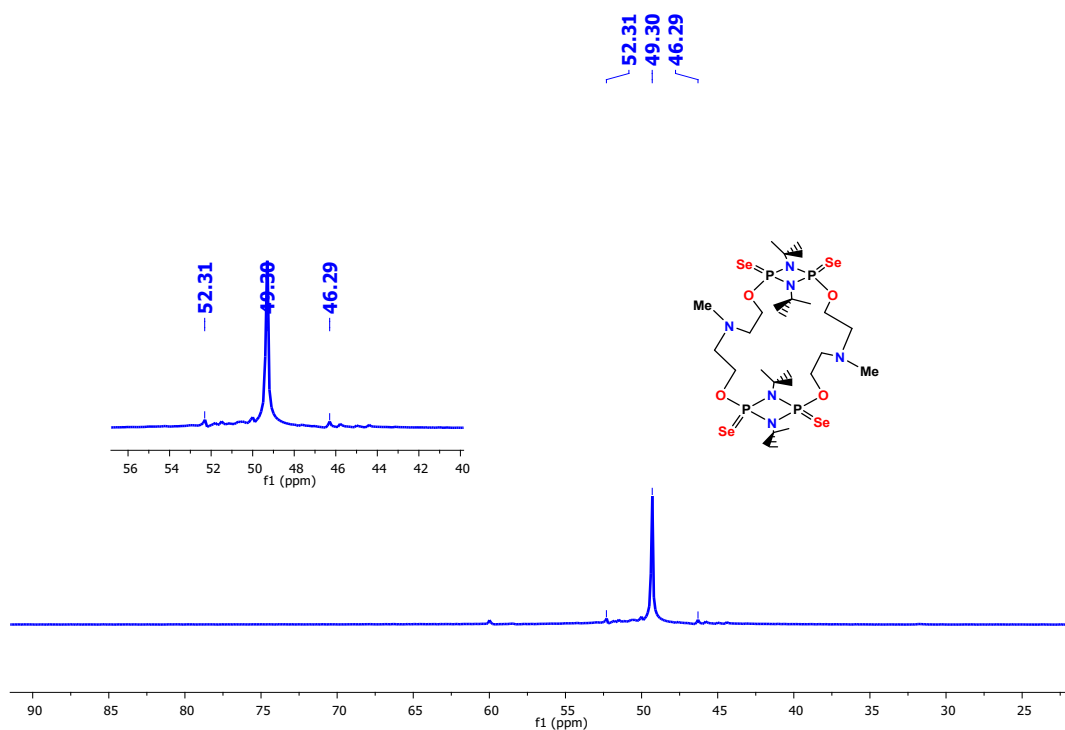


Fig.S26 $^{31}\text{P}\{^1\text{H}\}$ NMR (162 MHz, C_6D_6) spectrum of $\{(\text{Se}=\text{P}(\mu\text{-N}^t\text{Bu})_2\}\}_2\{\text{O}(\text{CH}_2)_2\text{N}(\text{Me})(\text{CH}_2)_2\text{O}\}_2$ (7), inset shows the satellites due to ^{77}Se .

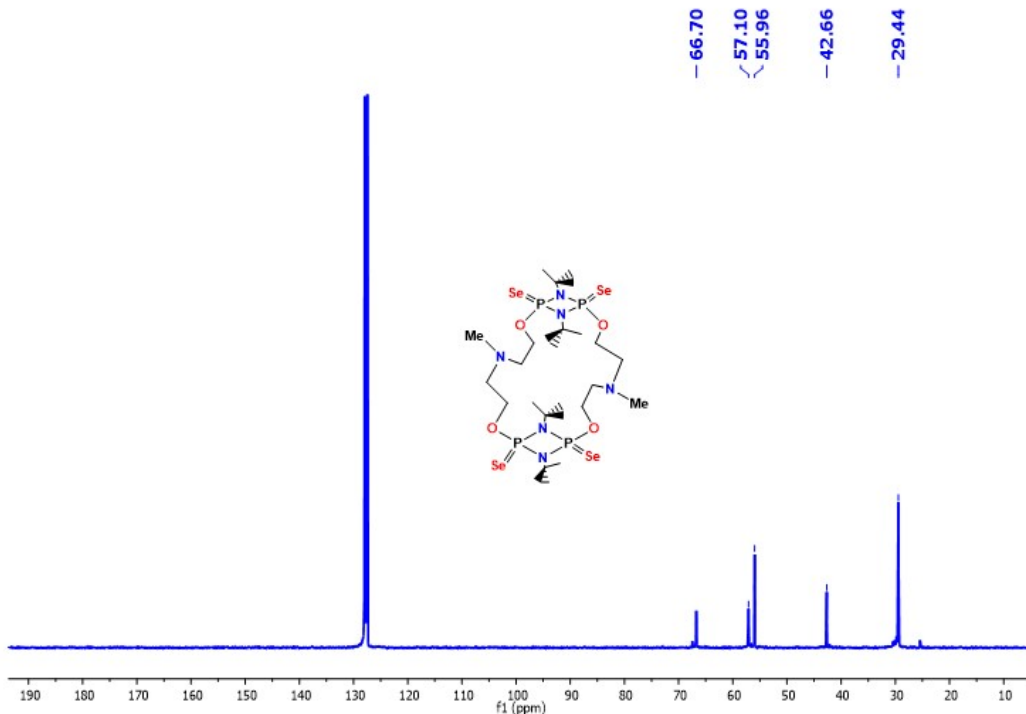


Fig.S27 $^{13}\text{C}\{\text{H}\}$ NMR (100 MHz, C_6D_6) spectrum of $[(\text{Se}=\text{P}(\mu\text{-N}^t\text{Bu})_2\{\text{O}(\text{CH}_2)_2\text{N}(\text{Me})(\text{CH}_2)_2\text{O}\}]_2$ (**7**).

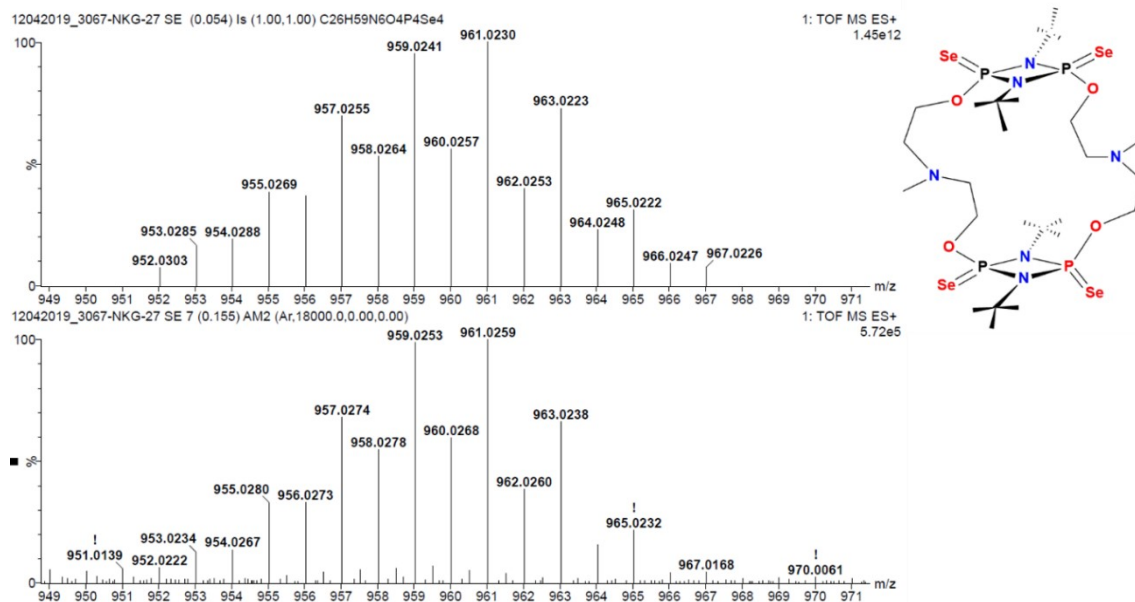


Fig.S28 HRMS spectrum of $[(\text{Se}=\text{P}(\mu\text{-N}^t\text{Bu})_2\{\text{O}(\text{CH}_2)_2\text{N}(\text{Me})(\text{CH}_2)_2\text{O}\}]_2$ (**7**).

Heteronuclear NMR spectra of $[(\text{Se}=\text{P}(\mu\text{-N}^t\text{Bu})_2\{\text{O}(\text{CH}_2)_2\text{N}(\text{Ph})(\text{CH}_2)_2\text{O}\}]_2$ (8)

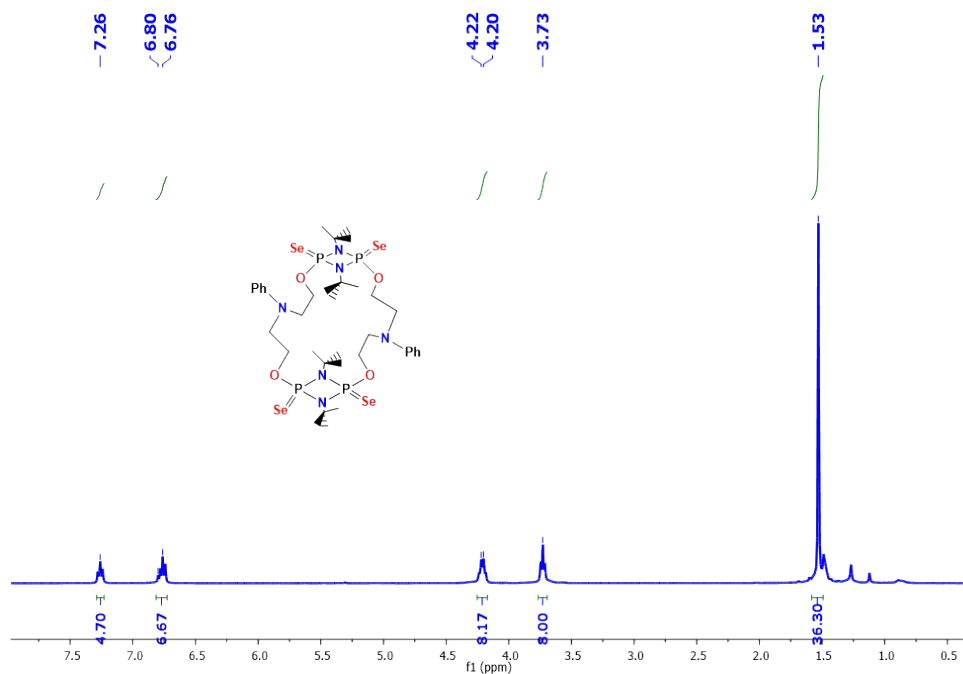


Fig.S29 ^1H NMR (400 MHz, CDCl_3) spectrum of $[(\text{Se}=\text{P}(\mu\text{-N}^t\text{Bu})_2\{\text{O}(\text{CH}_2)_2\text{N}(\text{Ph})(\text{CH}_2)_2\text{O}\}]_2$ (8).

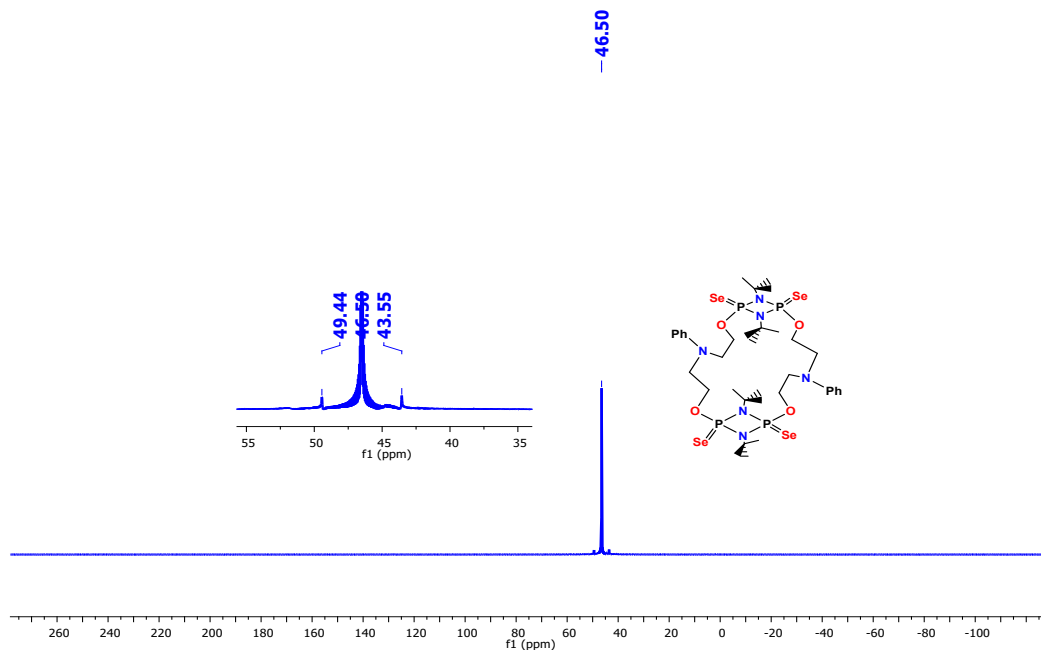


Fig.S30 $^{31}\text{P}\{\text{H}\}$ NMR (162 MHz, CDCl_3) spectrum of $[(\text{Se}=\text{P}(\mu\text{-N}^t\text{Bu})_2\{\text{O}(\text{CH}_2)_2\text{N}(\text{Ph})(\text{CH}_2)_2\text{O}\}]_2$ (8), inset shows the satellites due to ^{77}Se .

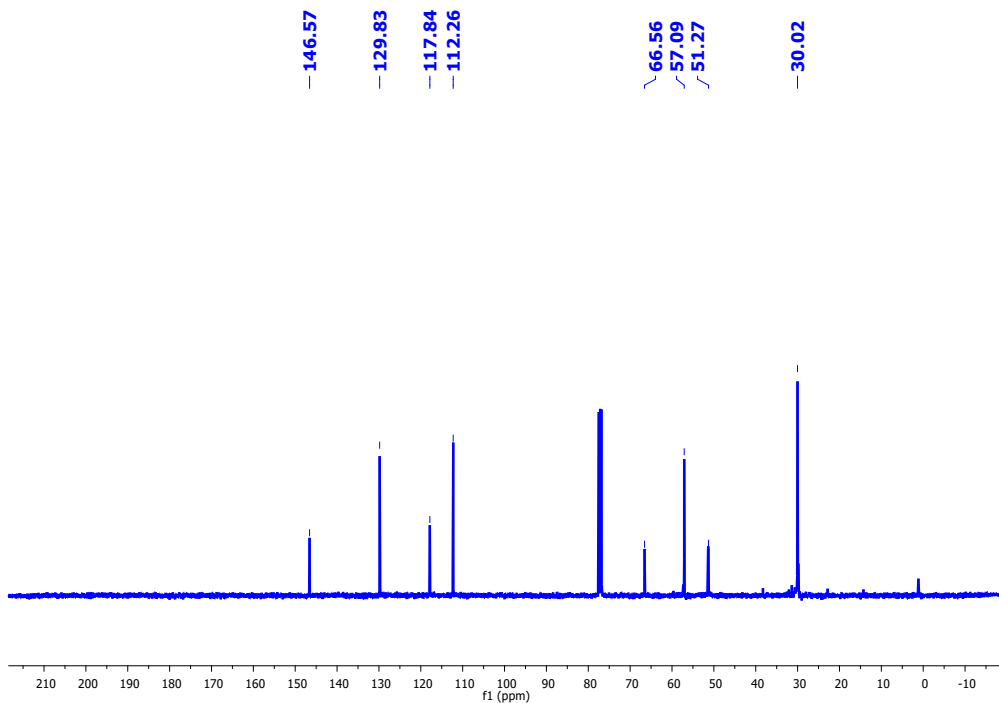


Fig.S31 $^{13}\text{C}\{\text{H}\}$ NMR (100 MHz, CDCl_3) spectrum of $[\{(\text{Se=})\text{P}(\mu\text{-N}^t\text{Bu})\}_2\{\text{O}(\text{CH}_2)_2\text{N}(\text{Ph})(\text{CH}_2)_2\text{O}\}]_2$ (**8**).

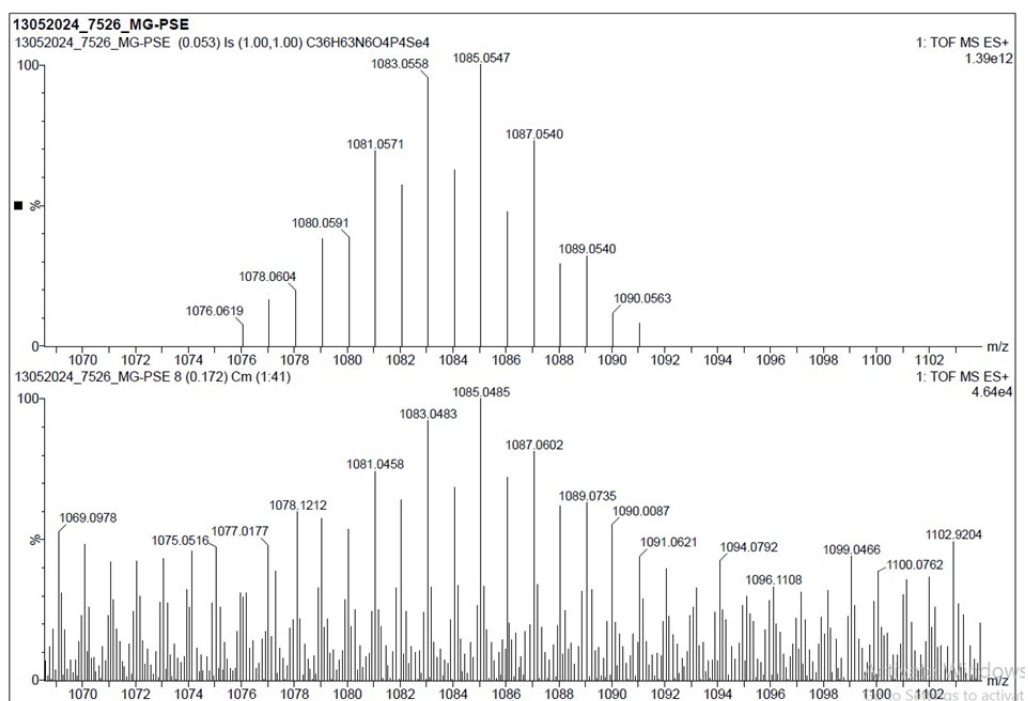


Fig.S32 HRMS spectrum of $[\{(\text{Se=})\text{P}(\mu\text{-N}^t\text{Bu})\}_2\{\text{O}(\text{CH}_2)_2\text{N}(\text{Ph})(\text{CH}_2)_2\text{O}\}]_2$ (**8**).

Heteronuclear NMR spectra of $[(\text{BH}_3)\text{P}(\mu\text{-N}^t\text{Bu})_2\{\text{O}(\text{CH}_2)_2\text{N}(\text{BH}_3)(\text{Me})(\text{CH}_2)_2\text{O}\}]_2$ (9)

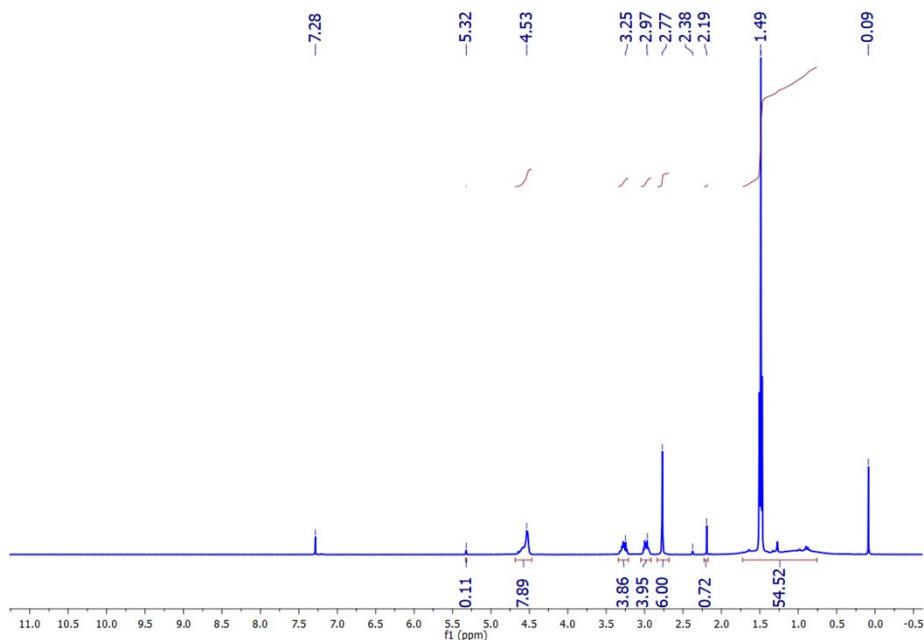


Fig.S33 ¹H NMR (400 MHz, CDCl₃) spectrum of $[(\text{BH}_3)\text{P}(\mu\text{-N}^t\text{Bu})_2\{\text{O}(\text{CH}_2)_2\text{N}(\text{BH}_3)(\text{Me})(\text{CH}_2)_2\text{O}\}]_2$ (9).

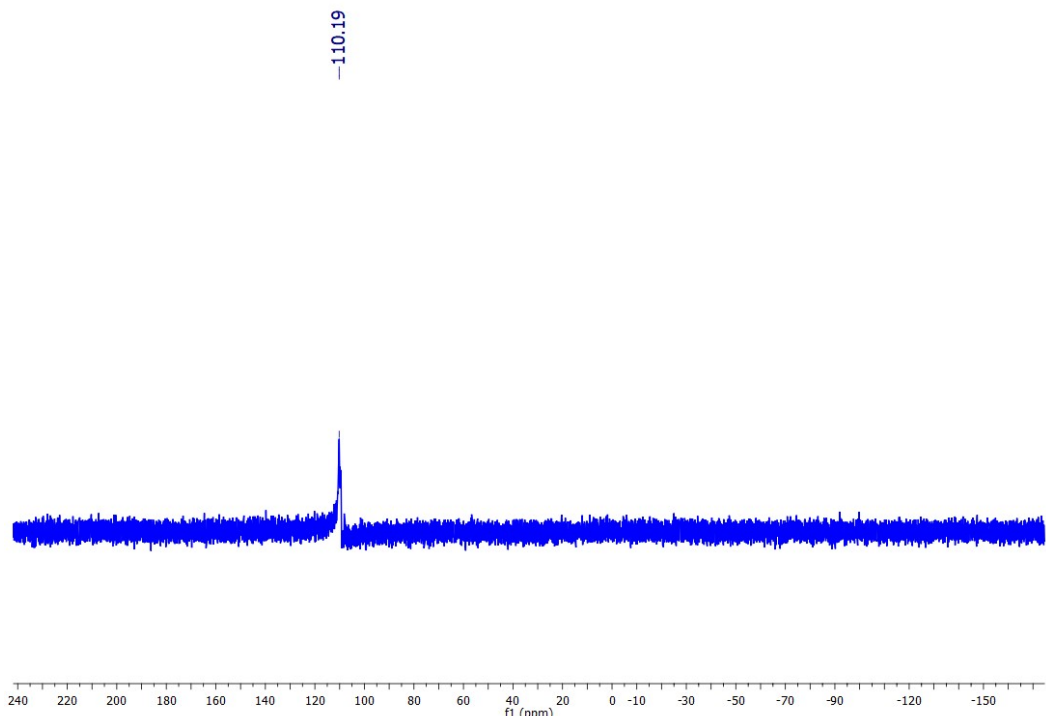


Fig.S34 ³¹P{¹H} NMR (162 MHz, CDCl₃) spectrum of $[(\text{BH}_3)\text{P}(\mu\text{-N}^t\text{Bu})_2\{\text{O}(\text{CH}_2)_2\text{N}(\text{BH}_3)(\text{Me})(\text{CH}_2)_2\text{O}\}]_2$ (9).

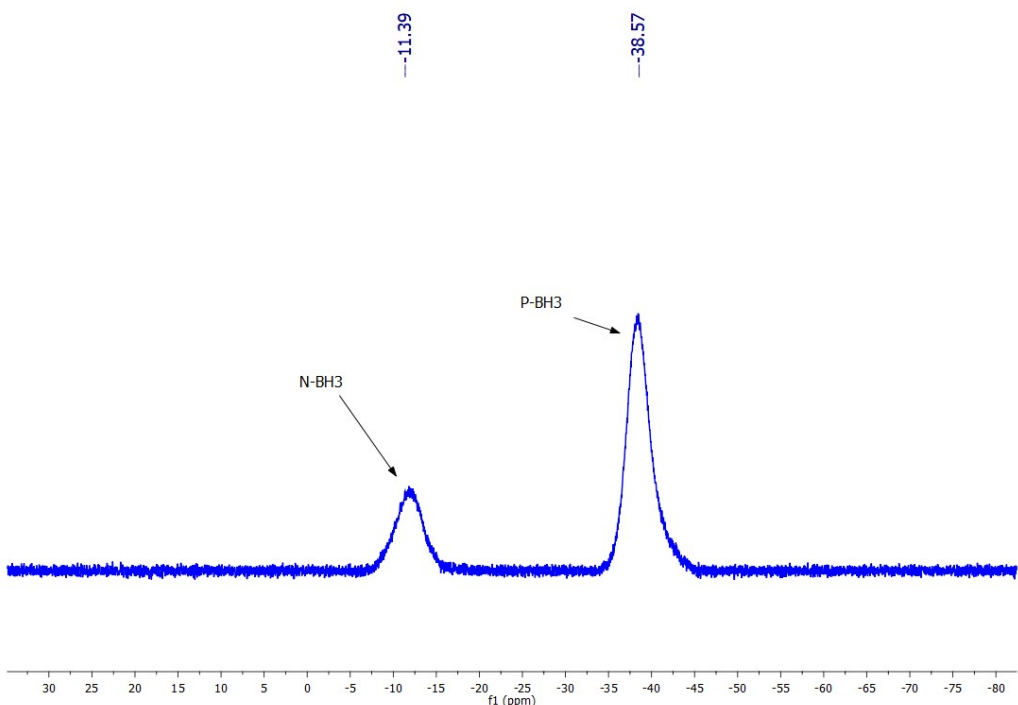


Fig.S35 ^{11}B NMR (128.4 MHz, CDCl_3) spectrum of $[\{(BH_3)P(\mu\text{-}N^t\text{Bu})\}_2\{O(CH_2)_2N(BH_3)(Me)(CH_2)_2O\}]_2$ (**9**).

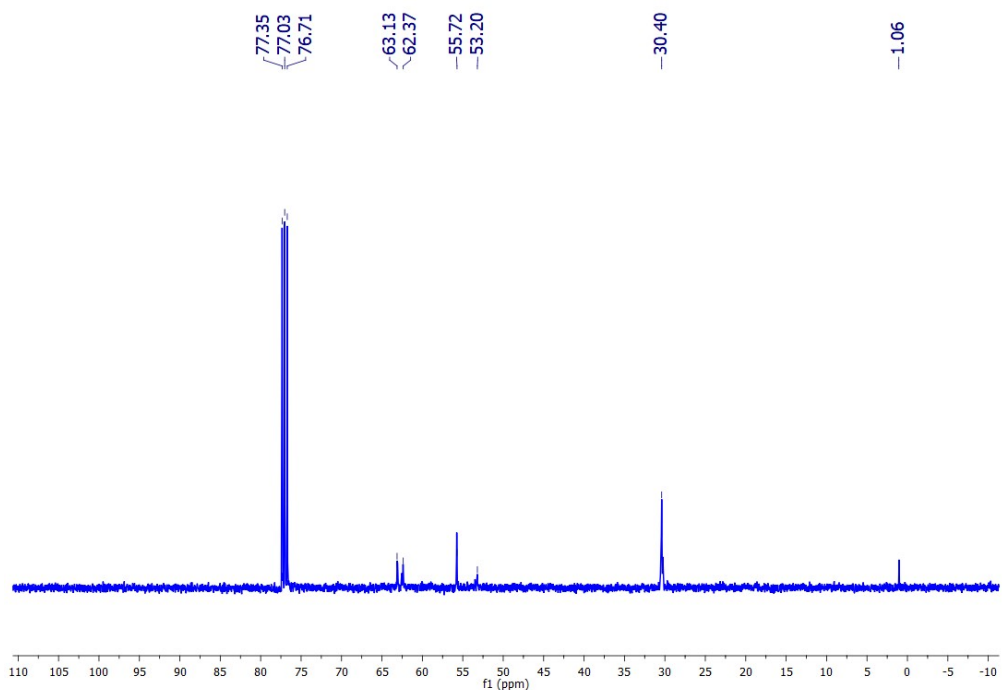


Fig.S36 $^{13}\text{C}\{^1\text{H}\}$ NMR (100 MHz, CDCl_3) spectrum of $[\{(BH_3)P(\mu\text{-}N^t\text{Bu})\}_2\{O(CH_2)_2N(BH_3)(Me)(CH_2)_2O\}]_2$ (**9**).

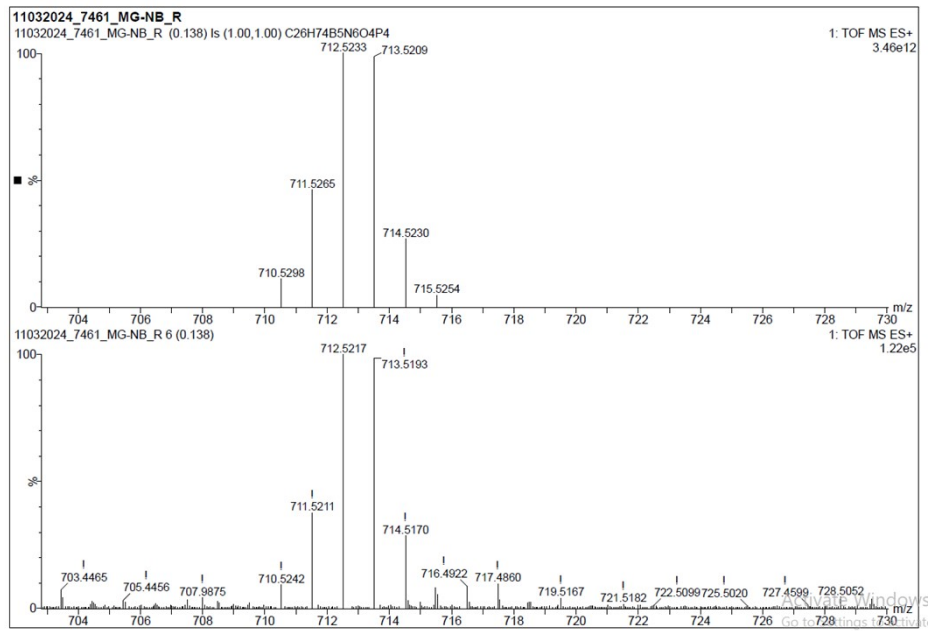


Fig.S37 HRMS spectrum of $[\{(BH_3)P(\mu\text{-}N^tBu)\}_2\{O(CH_2)_2N(BH_3)(Me)(CH_2)_2O\}]_2$ (**9**).

Heteronuclear NMR spectra of $[\{(BH_3)P(\mu\text{-}N^tBu)\}_2\{O(CH_2)_2N(Ph)(CH_2)_2O\}]_2$ (**10**)

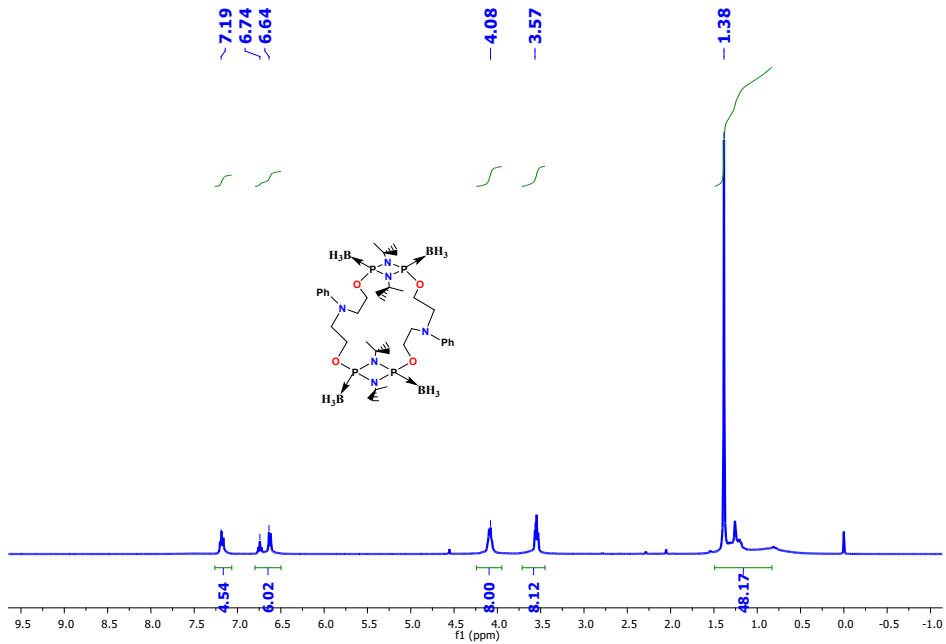


Fig.S38 1H NMR (400 MHz, $CDCl_3$) spectrum of $[\{(BH_3)P(\mu\text{-}N^tBu)\}_2\{O(CH_2)_2N(Ph)(CH_2)_2O\}]_2$ (**10**).

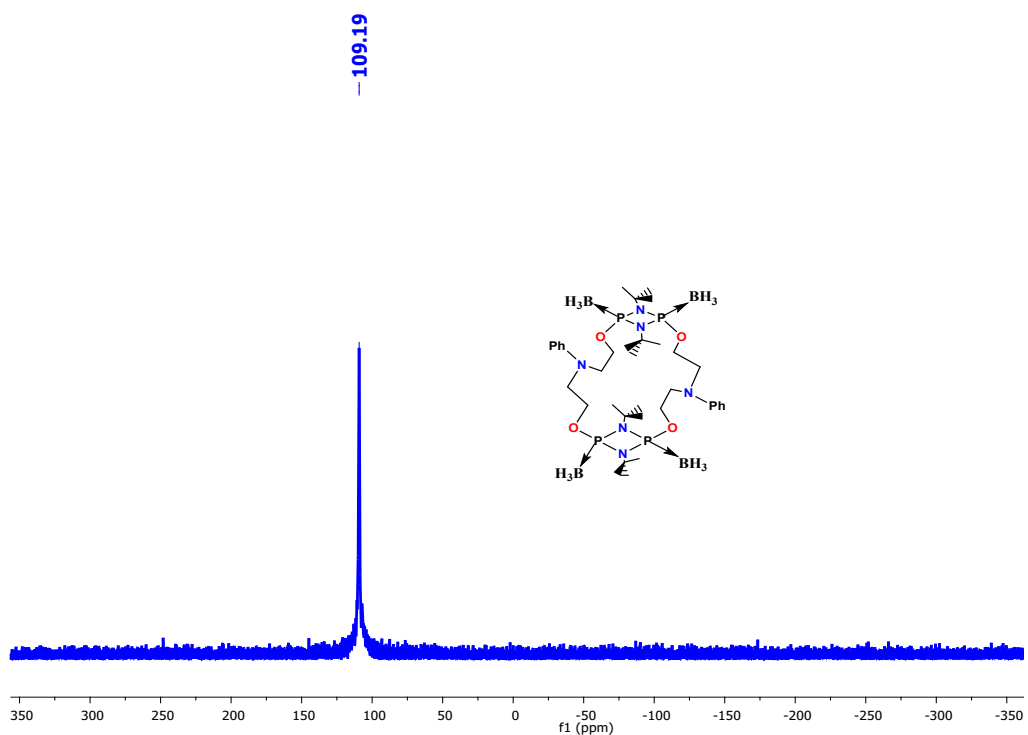


Fig.S39 $^{31}\text{P}\{\text{H}\}$ NMR (162 MHz, CDCl_3) spectrum of $[\{(BH_3)\text{P}(\mu\text{-N}^t\text{Bu})\}_2\{O(CH_2)_2\text{N}(\text{Ph})(CH_2)_2\text{O}\}]_2$ (**10**).

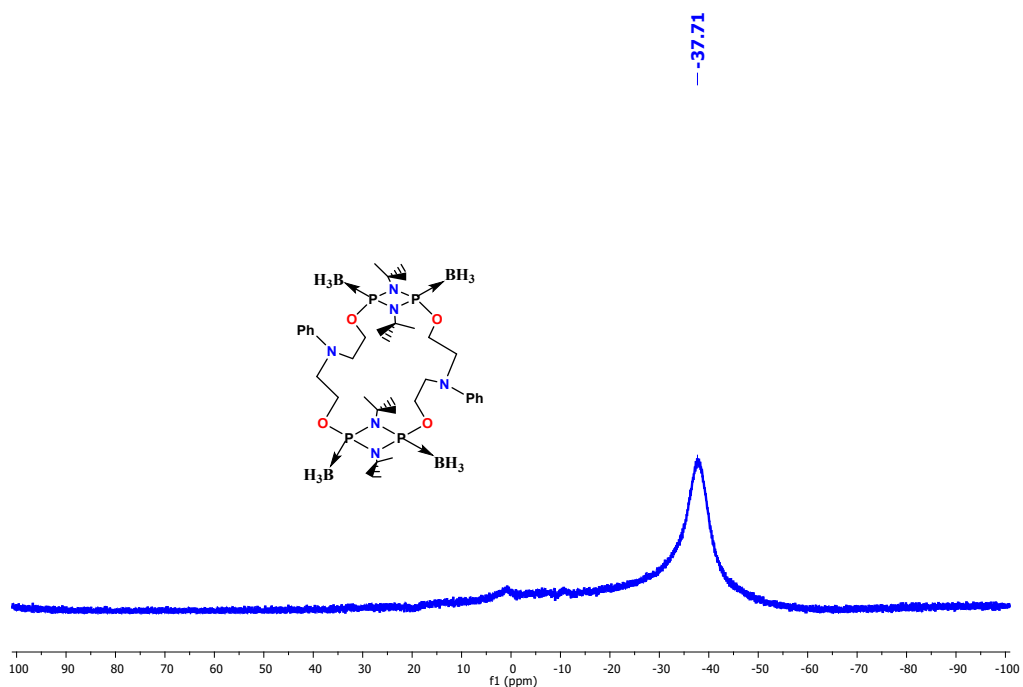


Fig.S40 ^{11}B NMR (128.4 MHz, CDCl_3) spectrum of $[\{(BH_3)\text{P}(\mu\text{-N}^t\text{Bu})\}_2\{O(CH_2)_2\text{N}(\text{Ph})(CH_2)_2\text{O}\}]_2$ (**10**).

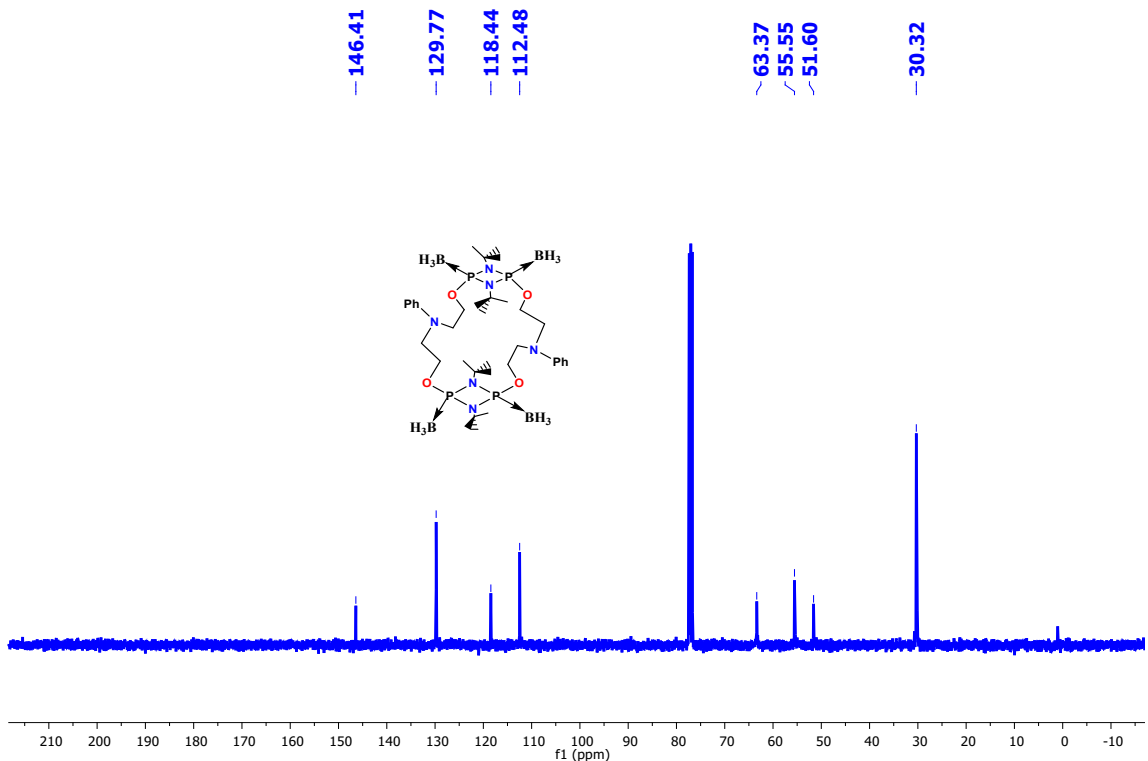


Fig.S41 $^{13}\text{C}\{\text{H}\}$ NMR (100 MHz, CDCl_3) spectrum of $[\{(\text{BH}_3)\text{P}(\mu-\text{N}^t\text{Bu})\}_2\{\text{O}(\text{CH}_2)_2\text{N}(\text{Ph})(\text{CH}_2)_2\text{O}\}]_2$ (**10**).

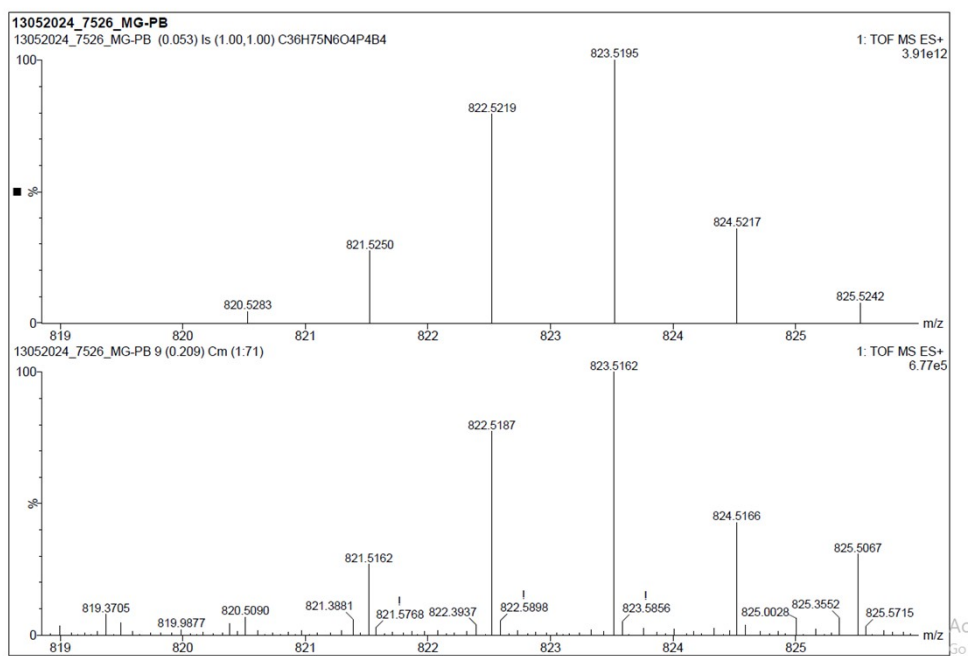


Fig.S42 HRMS spectrum of $[\{(\text{BH}_3)\text{P}(\mu-\text{N}^t\text{Bu})\}_2\{\text{O}(\text{CH}_2)_2\text{N}(\text{Ph})(\text{CH}_2)_2\text{O}\}]_2$ (**10**).

2. Crystal Data and Refinement Details of Compounds 1-3, 8 and 9

Single-crystal X-ray diffraction data for macrocycles **1-3**, **8**, and **9** were collected on a Rigaku XtaLAB mini diffractometer equipped with a Mercury375M CCD detector. Data were acquired using MoK α radiation ($\lambda = 0.71073 \text{ \AA}$) via omega scans. The detector distance was maintained at 49.9 mm throughout the data collection, and the detector was positioned at a fixed 2θ angle of 29.85° for all datasets. Data collection and reduction were performed using CrysAlisPro 1.171.38.46. The crystal structures were solved using the OLEX2¹ package with the SHELXT algorithm², and the refinement was carried out using SHELXL³. All non-hydrogen atoms were refined anisotropically. All the H and D atoms were geometrically fixed and refined using the riding model. Figures were generated using Mercury 2020.3.0. Geometric data were extracted from the CIF.

The asymmetric unit of compound **1** contains half of the molecule of macrocycle, and the other half is generated by inversion symmetry.

The asymmetric unit of compound **2** contains half of the molecule of macrocycle, and the other half is generated by inversion symmetry. One of the 'Bu groups in **2** was found to be disordered. These disordered atoms were refined with the use of PART and EADP commands.

The asymmetric unit of compound **3** consists of two distinct half molecules along with two molecules of THF and two molecules of the *m*-chlorobenzoic acid in the crystal lattice. Further analysis revealed that one THF moiety exhibited static disorder, which was effectively addressed using the PART and EADP commands.

The asymmetric unit of compound **8** contains half of the molecule of macrocycle along with a C₆D₆ molecule, and another half is generated by inversion symmetry.

The asymmetric unit of compound **9** contains half of the molecule of macrocyclic borane-adduct along with a DCM molecule and an uncharacterized solvent molecule in the crystal lattice. DCM molecule in **9** was found to be disordered. These disordered atoms were refined using the appropriate PART, EADP, and EXYZ commands. While there were attempts to model the structure of the unknown solvent molecule in **9**, we were not able to unequivocally refine it, so it was masked using the OLEX2¹. A solvent mask calculates 20 electrons and 58 (\AA^3) of volume in a unit cell in an asymmetric unit.

Table 1. Crystallographic data for compounds **1**, **2**, **3**, **8**, and **9**.

Compound^[a]	1	2	3·(THF)₂(<i>m</i>-Cl-C₆H₅O₂)₂	8·(C₆D₆)₂	9·(CH₂Cl₂)₂
Chemical formula	C ₂₆ H ₅₈ N ₆ O ₄ P ₄	C ₃₆ H ₆₂ N ₆ O ₄ P ₄	C ₄₈ H ₈₄ Cl ₂ N ₆ O ₁₄ P ₄	C ₄₈ H ₆₂ D ₁₂ N ₆ O ₄ P ₄ Se ₄	C ₂₈ H ₈₀ N ₆ O ₄ P ₄ B ₆ Cl ₄
Molar mass	642.66	766.79	1163.99	1250.92	895.52
Crystal system	monoclinic	triclinic	triclinic	monoclinic	monoclinic
Space group	<i>P</i> 2 ₁ / <i>c</i>	<i>P</i> 1̄	<i>P</i> 1̄	<i>P</i> 2 ₁ / <i>c</i>	<i>P</i> 2 ₁ / <i>n</i>
T [K]	100.00	250.01(10)	99.99(10)	200.00(10)	293(2)
a [Å]	9.4422(16)	9.4064(5)	14.2255(7)	13.0929(8)	9.4889(7)
b [Å]	18.041(3)	9.6314(6)	15.05329(7)	13.8043(7)	17.3728(11)
c [Å]	12.769(2)	12.6177(7)	15.8213(8)	16.9771(13)	16.2634(10)
α [°]	90	74.121(5)	94.818(4)	90	90
β [°]	126.539(2)	82.724(5)	99.230(4)	111.913(8)	93.963(6)
γ [°]	90	83.213(5)	115.342(4)	90	90
V [Å ³]	1747.6(5)	1086.46(11)	2977.7(3)	2846.7(3)	2674.6(3)
Z	2	1	2	2	2
ρ (calcd.) [g·cm ⁻³]	1.225	1.172	1.298	1.459	1.112
μ(Mo-K _α) [mm ⁻¹]	0.255	0.215	0.280	2.735	0.375
Reflections collected	7398	13771	36012	10513	19466
Independent reflections	3039	3838	10511	5045	4738
Data/restraints/ parameters	3039/0/188	3838/0/220	10511/1/661	5045/0/274	4738/12/276
R ₁ ,wR ₂ [I>2σ(I)] ^[a]	0.0636, 0.1891	0.0813, 0.2108	0.0716, 0.1884	0.0516, 0.1413	0.0801, 0.2126
R ₁ , wR ₂ (all data) ^[a]	0.0682, 0.1919	0.1129, 0.2518	0.1019, 0.2351	0.0710, 0.1620	0.1069, 0.2466
GOF	1.098	1.061	1.053	1.087	1.058
CCDC No.	2403424	2403425	2403426	2403427	2403428

[a] R₁ = Σ ||F_o|| - ||F_c|| / Σ ||F_o||, wR₂ = [Σw(||F_o²|| - ||F_c²||)² / Σw||F_o²||]^{1/2}

3. References:

1. O. V. Dolomanov, L. J. Bourhis, R. J. Gildea, J. A. K. Howard, and H. Puschmann, *J. Appl. Cryst.* 2009, **42**, 339-341.
2. G. M. Sheldrick, *Acta Cryst., Sect. A*, 2015, **71**, 3-8.
3. G. M. Sheldrick, *Acta Cryst., Sect. A*, 2008, **64**, 112-122